

Armed Services Technical Information Agency

AD

18819

NOTICE: WHEN GOVERNMENT OR OTHER DRAWINGS, SPECIFICATIONS OR OTHER DATA ARE USED FOR ANY PURPOSE OTHER THAN IN CONNECTION WITH A DEFINITELY RELATED GOVERNMENT PROCUREMENT OPERATION, THE U. S. GOVERNMENT THEREBY INCURS NO RESPONSIBILITY, NOR ANY OBLIGATION WHATSOEVER; AND THE FACT THAT THE GOVERNMENT MAY HAVE FORMULATED, FURNISHED, OR IN ANY WAY SUPPLIED THE SAID DRAWINGS, SPECIFICATIONS, OR OTHER DATA IS NOT TO BE REGARDED BY IMPLICATION OR OTHERWISE AS IN ANY MANNER LICENSING THE HOLDER OR ANY OTHER PERSON OR CORPORATION, OR CONVEYING ANY RIGHTS OR PERMISSION TO MANUFACTURE, USE OR SELL ANY PATENTED INVENTION THAT MAY IN ANY WAY BE RELATED THERETO.

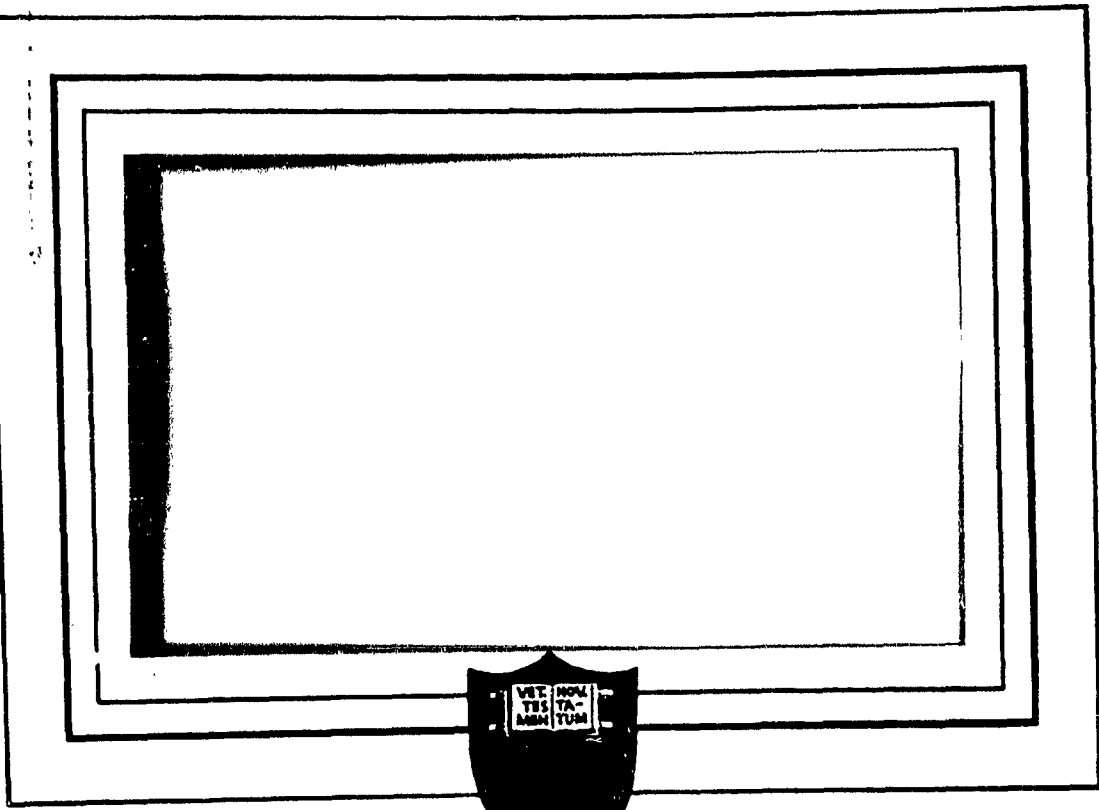
Reproduced by
DOCUMENT SERVICE CENTER
KNOTT BUILDING, DAYTON, 2, OHIO

UNCLASSIFIED

NOTICE: THIS DOCUMENT CONTAINS INFORMATION AFFECTING THE NATIONAL DEFENSE OF THE UNITED STATES WITHIN THE MEANING OF THE ESPIONAGE LAWS, TITLE 18, U.S.C., SECTIONS 793 and 794. THE TRANSMISSION OR THE REVELATION OF ITS CONTENTS IN ANY MANNER TO AN UNAUTHORIZED PERSON IS PROHIBITED BY LAW.

AD No. 18 819

ASTIA FILE COPY



PRINCETON UNIVERSITY
DEPARTMENT OF AERONAUTICAL ENGINEERING

FURTHER CORRELATION OF OBSERVED AND
THEORETICAL HELICOPTER DYNAMIC LONGITUDINAL
RESPONSE CHARACTERISTICS

Edward Seckel

Aeronautical Engineering Report No. 227

March 31, 1953

AIR FORCE CONTRACT NO. AF 33(616)-114
EXPENDITURE ORDER NO. R-458-393 SR-1g

Reproduction of this matter in any form, by other than the cognizant governmental activity, is not authorized, except by specific approval of the cognizant governmental activity.

The work reported herein was sponsored by the Aerodynamics Branch of the Aircraft Laboratory, Air Materiel Command, Wright-Patterson Air Force Base, Dayton, Ohio, under the terms of Personal Services Contract No. AF 33 (616) -114, and was administered by Mr. Lindenbaum of that organization.

TABLE OF CONTENTS

	Page No.
I. Summary	1.
II. Introduction	2.
III. Symbols	3.
IV. Theory	10.
A. The Equations of Motion	10.
B. The Analogue Computations	18.
C. Simplified Equations of Motion	19.
D. Frequency Response	21.
V. Results and Discussion	24.
A. Transient Pulse Responses	24.
B. Stability Derivatives	25.
C. Bar Damper Settings	29.
D. Individual Transient Responses	30.
E. Frequency Response	32.
VI. Conclusions	33.
VII. List of References	34.
VIII. Appendix - The Bar Equation	35.
IX. List of Figures	38.

I. SUMMARY

Extended attempts are made to correlate previously obtained helicopter longitudinal dynamic response data with theoretical predictions. The helicopter was a Bell, H-13 type, incorporating the stabilizer bar. The motions were in response to a pulse-type stick movement.

Satisfactory correlation is obtained with either fairly complete equations of motion or greatly simplified ones. The shortened equations are simple enough that even hand calculation of transient or frequency responses is feasible. The attendant sacrifice in accuracy is shown to be negligible compared to the errors due to inaccurate estimation of the important stability derivatives.

Strong evidence is given that the fuselage moment derivatives are greatly different from theoretical predictions, and that they alone account for the helicopter's dynamic stability in forward flight. It is also indicated that, at least in the low speed range, the lift derivatives are inadequately predicted by theory, with the discrepancies probably associated with the imperfect understanding of the downwash behavior.

Re-examination of the data for other than standard damper settings indicates that loosening the bar damper setting does not materially affect the damping of the phugoid mode, but rather affects the relative excitation of the various modes of response in such a way as to give the impression of increased stability. Although the inability of the stabilizer bar to dampen the phugoid is predicted by theory, the other effects are not sufficiently explained. A more detailed theoretical treatment of the stabilizer bar failed to produce any improvement, and it is assumed that non-linear damper characteristics are responsible.

II. Introduction

A research program of flight-testing a Bell H-13 helicopter for its longitudinal dynamic response characteristics was accomplished by the Cornell Aeronautical Laboratory, Inc., completed in March, 1951. It was the objective of that program to demonstrate the feasibility of obtaining the dynamic stability characteristics of a helicopter, and to correlate these with the predictions of a simple theory. The results were presented in a data report (Reference 1) and an analysis report (Reference 2). The analysis was somewhat limited by the time available, and the attempts to correlate theoretical and observed responses were inconclusive.

It was believed highly desirable to make further attempts at correlation of theory and experiment, in order to provide a more positive evaluation of the theory. Particularly promising areas for further investigation were as outlined below.

- A. For most of the calculations of Reference 2, rather simplified equations of motion were used. It was desirable to investigate more fully the effects of those simplifications, and to show whether the discrepancies were assessable to them.
- B. The comparison between theoretical and observed responses was originally on the basis of phugoid period and damping. This alone gave little feeling for flying qualities, and it was desirable to compare the entire transient responses, including the amplitudes of response, and the short-period mode. Work on these two aspects of the problem would be greatly facilitated by an analogue computer, which, fortunately, could be made available. The length of hand calculations of this sort would have been prohibitive.
- C. Since the work of Reference 2 indicated that values of the stability derivatives required for agreement were considerably different from theoretical predictions, any independent method for their evaluation would be important. Particularly it was recognized that a method for evaluating the fuselage moment derivatives, from the steady trim data could be developed.
- D. The comparison of theoretical and derived frequency response data was especially abbreviated in the previous work, and it was desirable to calculate the frequency responses more fully than had previously been attempted for comparison with the test data.

The material presented in this report is primarily centered in the areas outlined above, and may be regarded as an extension of the data analysis given in Reference 2.

III. Symbols

The symbols used in this report are the same as in Reference 2. They are repeated here for convenience.

A. Forces and Moments

L	Lift force, perpendicular to relative wind, positive up.
D	Drag force, parallel to relative wind, positive to rear.
M	Pitching moment, positive nose up.
T	Thrust, parallel to axis of no feathering, positive up.
H	"Horizontal" force, perpendicular to axis of no feathering, positive rearward.

$$L_u = \frac{1}{W} \frac{\partial L}{\partial u/V_0}$$

$$L_{\alpha} = \frac{1}{W} \frac{\partial L}{\partial \alpha}$$

non-dimensional
lift derivatives

$$D_u = \frac{1}{W} \frac{\partial D}{\partial u/V_0}$$

$$D_{\alpha} = \frac{1}{W} \frac{\partial D}{\partial \alpha}$$

non-dimensional
drag derivatives

$$D_{\alpha_1} = \frac{1}{W} \frac{\partial D}{\partial \alpha_1}$$

$$D_{\dot{\phi}} = \frac{1}{W} \frac{\partial D}{\partial \dot{\phi}}$$

3.

$$M_u = \frac{1}{Wh} \frac{\partial M}{\partial u}$$

$$M_\alpha = \frac{1}{Wh} \frac{\partial M}{\partial \alpha}$$

$$M_{\dot{\phi}} = \frac{1}{Wh} \frac{\partial M}{\partial \dot{\phi}}$$

$$M_{\alpha_1} = \frac{1}{Wh} \frac{\partial M}{\partial \alpha_1}$$

non-dimensional
moment derivatives

$$\bar{M}_u = \frac{1}{Wh} \frac{dM}{d u}$$

$$\bar{M}_\alpha = \frac{1}{Wh} \frac{dM}{d \alpha}$$

total derivatives

B. Physical Dimensions of the Helicopter

m	Mass of the helicopter
I_y	Helicopter pitching moment of inertia (slug = ft ²)
h	Height of rotor hub above helicopter center of gravity (ft.)

l	Distance of helicopter c.g. ahead of the initial position of the axis of no feathering
l_s	Distance of helicopter c.g. ahead of rotor shaft
b	Number of blades
Ω	Rotor speed, radians/sec.
R	Rotor radius, ft.
c	Blade chord, ft.
I_b	Blade moment of inertia, slug-ft. ²
I_s	Stabilizer bar moment of inertia
C	Stabilizer bar damping constant ft-#/rad./sec.
s	"Stability Ratio" - linkage ratio between stabilizer bar and blade pitch change
S_t	Tail area - square ft.
l_t	Tail length, measured from c.g. to c.p. of tail (ft.)
λ	Lock's blade inertia coefficient, $\lambda = \frac{\rho a c R^4}{I_b}$

C. Velocities and Angles

U	Speed of helicopter along the flight path - ft. per sec.
u	Increment of speed, $\Delta U = U - U_0$
α	Angle of attack of normal to axis of no feathering
α_1	Longitudinal flapping angle from axis of no feathering, positive if tip plane is tilted rearward
ϵ	Downwash angle, positive downward
γ	Flight path angle to the horizon, positive in climb

ϕ Pitch angle of fuselage, measured to a reference in the fuselage, normal to the initial position of the axis of no feathering.

ϕ_s Pitch angle of the fuselage, measured to the normal to the rotor shaft

The following are measured to a plane normal to rotor shaft:

α_s Angle of attack of the normal to the rotor shaft

β_s Blade flap angle, positive up

$$\beta_s = \alpha_{0s} - a_{1s} \cos \psi - b_{1s} \sin \psi \\ - \alpha_{2s} \cos 2\psi - b_{2s} \sin^2 \psi - \dots$$

For the 2 blade see-saw rotor, the even harmonics are zero.

a_{1s} Longitudinal blade flap, positive if tip path plane is tilted rearward.

A_s Blade pitch angle, positive for increased pitch

$$\theta_s = A_{0s} - A_{1s} \cos \psi - B_{1s} \sin \psi - \dots$$

A_{0s} Collective pitch

B_{1s} Longitudinal cyclic pitch, positive stick forward.

A_{1s} Lateral cyclic pitch, positive stick right.

For the Bell Helicopter,

$$\theta_s(\psi) = \nu_s(\psi) + s\eta_s(\psi + 90^\circ)$$

so that

$$B_{1s} = u_{1s} - s n_{1s}$$

$$A_{1s} = v_{1s} + s m_{1s}$$

ν_s Swash plate inclination

$$\nu_s = -v_{1s} \cos \psi - u_{1s} \sin \psi$$

u_{1s} Longitudinal control angle, positive stick forward.

v_{1s} Lateral control angle, positive stick right.

η_s Bar flap angle.

$$\eta_s(\psi_1) = -n_{1s} \cos \psi_1 - m_{1s} \sin \psi_1 \\ - n_{3s} \cos 3\psi_1 - m_{3s} \sin 3\psi_1 - \dots$$

where ψ_1 is the azimuth of the bar itself, and the even harmonics are zero.

n_{1s} Longitudinal bar flap-positive if bar tip plane is tilted rearward.

D. Aerodynamic Parameters

μ Advance ratio, $\mu = \frac{v}{\Omega R}$

λ	Inflow ratio, of resultant velocity along the axis of no feathering to the tip speed.
δ	Mean profile drag coefficient of rotor blades.
α	Slope of the rotor blade lift curve/rad.
α_t	Slope of the tail lift curve
σ	Solidity ratio, $\sigma = \frac{bc}{TR}$
k	Constant, $k = \frac{c_{D0}}{2C_T}$
C_T	Thrust coefficient, $C_T = \frac{T}{\rho(\pi R^2)(\Omega R)^2}$
R_g	Rotor gyroscopic coefficient, $R_g = \frac{I_g}{\Omega \delta}$

E. Miscellaneous

R	Total rotor damping in pitch parameter see Equation (9b)
R_0	Routh's discriminant
C_g	Stabilizer bar gyroscopic coefficient; $C_g = \frac{2I_s}{C}$
λ	Root of the stability characteristic equation
R_{cos}, R_{sin}	Dial readings of harmonic analyzer expressed in units of variable.
ω, A, b, T	Constants in expression (Equation 63, Ref. 2) for transient response.
ω	Frequency (rad/sec.) in sinusoidal frequency response calculations

F. Subscripts

()_r Of the rotor, viz. M_r

()_f

()_s

Of the fuselage, Viz. M_f

Measured to the rotor shaft, rather than to the initial position of the axis of no feathering.

IV. THEORY

The basic theory underlying the analysis here presented, is given in considerable detail in Reference 2, where equations of longitudinal motion for the helicopter are derived. It has been found convenient, however, to use those equations in slightly different form for the investigations herein, and it is therefore desirable to show how they are obtained from the work of Reference 2.

A. The Equations of Motion

1. The Drag Equation:

The drag equation is essentially in the form given by equation (8) of Reference 2. As before, the variation of drag with pitching, $D_{\dot{\phi}}$, has been disregarded; but in this new work, the possibility of fuselage drag change with angle of attack is allowed, and the assumption (p. 23 Reference 2) that the fuselage drag varies with the square of forward speed, is renounced. This more general treatment is made feasible by the further development of methods for evaluating these effects from the flight data. The methods used are described in a later section of the report. The drag equation is, then

$$(1) \quad \left(\frac{U_0}{g} d + D_u \right) \frac{u}{U_0} + D_{\alpha} \cdot \alpha_s + \phi + D_{a_1} \cdot a_1 \\ + S (1 + D_{\alpha_r}) \eta_{1s} = (1 + D_{\alpha_r}) u_{1s}$$

where the derivatives are

$$(1a) \quad D_u = \frac{1}{W} \frac{\partial D_f}{\partial u/U_0} + \alpha_0 \frac{1}{W} \frac{\partial T}{\partial u/U_0} + \frac{1}{W} \frac{\partial H}{\partial u/U_0}$$

$$(1b) \quad D_{\alpha} = \frac{1}{W} \frac{\partial D_f}{\partial \alpha_s} + \alpha_0 \frac{1}{W} \frac{\partial T}{\partial \alpha} + \frac{1}{W} \frac{\partial H}{\partial \alpha}$$

$$(1c) \quad D_{\alpha_r} = \alpha_0 \frac{1}{W} \frac{\partial T}{\partial \alpha} + \frac{1}{W} \frac{\partial H}{\partial \alpha}$$

$$(1d) \quad D_{a_1} = \frac{1}{W} \frac{\partial H}{\partial a_1}$$

In the previous work, the drag equation was replaced by a combination of the drag and moment equations. This is only fruitful if the fuselage effects are assumed simple, as in Reference 2, and in this more general treatment, it is more desirable to retain the form of equation (1).

2. The Lift Equation:

The lift equation is retained in the form previously given (Reference 2, Equation 7), and it is again assumed that the effects of fuselage lift and pitching are negligible. The result is repeated below.

$$(2) \quad L_u \frac{u}{U_0} + \left(\frac{U_0}{g} d + L_\alpha \right) \alpha_s - \frac{U_0}{g} d\phi$$

$$+ s L_\alpha n_{1s} = L_\alpha u_{1s}$$

where

$$(2a) \quad l_\alpha = \frac{1}{N} \frac{\partial T}{\partial u/U_0}$$

$$(2b) \quad L_\alpha = \frac{1}{N} \frac{\partial T}{\partial \alpha}$$

3. The Moment Equation:

The important moment equation is again equation 11 of Reference 2, in which the effect of pitching on apparent rotor forward speed is neglected:

$$(3) \quad M_u \frac{u}{U_0} + M_\alpha \alpha_s - \frac{I}{Wh} d^2 \phi + M_\beta \beta_1$$

$$+ s (1 + M_{\alpha r}) n_{1s} = (1 + M_{\alpha r}) u_{1s}$$

in which

$$(3a) \quad M_u = \frac{1}{Wh} \frac{\partial M_f}{\partial u/U_0} - \frac{l}{h} \cdot \frac{1}{W} \frac{\partial T}{\partial u/U_0} + \frac{1}{W} \frac{\partial H}{\partial u/U_0}$$

$$(3b) \quad M_\alpha = \frac{1}{Wh} \frac{\partial M_f}{\partial \alpha_s} - \frac{l}{h} \cdot \frac{1}{W} \frac{\partial T}{\partial \alpha} + \frac{1}{W} \frac{\partial H}{\partial \alpha}$$

$$(3c) \quad M_{\alpha_r} = - \frac{l}{h} \cdot \frac{1}{W} \frac{\partial T}{\partial \alpha} + \frac{1}{W} \frac{\partial H}{\partial \alpha}$$

$$(3d) \quad M_{a_1} = \frac{1}{W} \frac{\partial H}{\partial a_1}$$

4. The Flap Equation:

This is the same as equation 13 of Reference 2, in which, again the effect of helicopter pitching on rotor airspeed is disregarded:

$$(4) \quad a_{1u} \frac{u}{U_0} + a_{1\alpha} \alpha_s - R_g d \phi - (R_g d + 1) a_1 \\ + (-s R_g d + s a_{1\alpha}) \eta_{1s} = (-R_g d + a_{1\alpha}) u_{1s}$$

where

$$(4a) \quad a_{1u} = \frac{\partial a_1}{\partial u/U_0}$$

$$(4b) \quad a_{1\alpha} = \frac{\partial a_1}{\partial \alpha}$$

and the gyroscopic rotor coefficient, R_g , is given by

$$(4c) \quad E_g = \frac{16}{r\Omega}$$

5. The Bar Equation:

The simplified bar equation (15, Reference 2) is retained, and quoted here only for convenience:

$$(5) \quad C_g d\phi + (C_g d + 1) \cdot n_{1s} = 0$$

where

$$(5a) \quad C_g = \frac{2I_s}{C}$$

The effects of concentrating the bar mass at the bar tips, rather than in a ring of the bar diameter, have been examined, and are reported in the Appendix. Although the more exact expressions there derived are somewhat different from the above, it is shown that they are not significantly so, and equation (5) is retained.

The foregoing equations suffice to calculate the helicopter response to a movement of the cyclic control, u_{1s} , providing a means is at hand for the estimation of the rotor and fuselage force and moment derivatives.

The evaluation of the rotor forces is purely theoretical, as in Reference 2. Two discrepancies may be noted between the expressions below and Reference 2, in $\frac{1}{W} \frac{\partial T}{\partial u/V_0}$ and $\frac{1}{W} \frac{\partial H}{\partial u/V_0}$.

These arise from the use of a better expression for $\frac{\partial \lambda}{\partial \mu}$ (Ref. 2, p. 26) as follows,

$$\frac{\partial \lambda}{\partial \mu} = \frac{\lambda}{\mu} + \frac{C_T}{\mu^2}$$

and equations (6) and (6c) below may be regarded as refinements of (30) and (33) of Reference 2. For the current work, the re-evaluation of $\frac{1}{W} \frac{\partial T}{\partial u/V_0}$ is important; but with the method described later

for evaluating D_{u_f} and M_{u_f} from flight data, the term $\frac{1}{W} \frac{\partial H}{\partial u/V_0}$ exactly cancels out of equations (1a) and (3a), and errors in its estimation are therefore of no significance.

Formulas for the rotor force derivatives are collected below, corrected as discussed above:

$$(6) \quad \frac{1}{W} \frac{\partial T}{\partial u_0} = \frac{3\mu^2 + \frac{\kappa\lambda}{2} \left(1 - \frac{3}{2}\mu^2\right) + \frac{\kappa C_T}{2\mu}}{1 + \frac{\alpha\sigma}{\delta\mu}}$$

$$(6a) \quad \frac{1}{W} \frac{\partial T}{\partial x} = \frac{\frac{\mu k}{2}}{1 + \frac{\alpha\sigma}{\delta\mu}}$$

$$(6b) \quad \frac{1}{W} \frac{\partial T}{\partial a_1} = 0$$

$$(6c) \quad \frac{1}{W} \frac{\partial H}{\partial u_0} = -3\mu\lambda \left(1 - \frac{\kappa C_T}{4\mu}\right) - \frac{3}{2} C_T \left(1 + \frac{\kappa C_T}{4\mu}\right) \\ + k \left\{ \frac{\delta}{2a} \mu + \frac{1}{4} \mu a_1^2 + \frac{3}{4} \mu \lambda^2 \left(1 - \frac{\kappa C_T}{\delta\mu}\right) + \frac{3}{4} \lambda a_1 \left(1 - \frac{\kappa C_T}{4\mu}\right) \right. \\ \left. + \frac{3}{3} \lambda C_T \left(1 + \frac{\kappa C_T}{2\mu}\right) + \frac{3}{4} \frac{a_1 C_T}{\mu} \left(1 + \frac{\kappa C_T}{4\mu}\right) \right\}$$

$$(6d) \quad \frac{1}{W} \frac{\partial H}{\partial \alpha} = \frac{-\frac{3}{2}\mu^2 + \frac{3}{4}\mu k (\mu\lambda + a_1)}{1 + \frac{\alpha\sigma}{\delta\mu}}$$

$$(6e) \quad \frac{1}{W} \frac{\partial H}{\partial a_1} = 1 - \frac{3}{2}\mu^2 + \frac{\kappa}{4} \left[\lambda (1 + 3\mu^2) + 2\mu a_1 \right]$$

The a_1 derivatives in equations (6a) and (6b) are quoted directly from Reference 2,

$$(6f) \quad \frac{\partial a_1}{\partial u_0} = a_1 + \frac{2\mu\lambda}{1 + \frac{\alpha\sigma}{\delta\mu}}$$

$$(6g) \quad \frac{\partial a_1}{\partial \alpha} = \frac{2\mu^2}{1 + \frac{\alpha\sigma}{\theta\mu}}$$

It should again be remarked that in the expressions (6) through (6g), the collective pitch, θ , has carefully been eliminated to help avoid large errors in the derivatives due to small errors in its measurement and inconsistencies in the original thrust equation.

It remains now to evaluate the fuselage force and moment derivatives. These had previously been shown to be very important, and their estimation on purely theoretical grounds is especially difficult. Even available wind-tunnel data (Reference 4) was unsatisfactory due to the small scale and the absence of the rotor and horizontal tail. Scale effect and rotor downflow could be especially important in the case of the H-13 helicopter since the NACA (unpublished data) has shown that the fuselage characteristics depend critically on the exact shape of the large, bulbous, canopy; and are even widely different between ships, due to manufacturing tolerances.

This situation led to the development of a method for evaluating these derivatives from steady trim data at different airspeeds and c.g. locations. Although the method suffers somewhat from a limited c.g. range in the tests, it is perhaps significant that it does predict the very stable fuselage angle-of-attack derivative required for correlation of the dynamic stability characteristics. The method was quoted in Reference 5, and a derivation of the equations is given below.

For a helicopter in trim, in steady flight, it can be shown, by taking moments about the c.g., that

$$M_f = -hH + Tl$$

where H and T are resolved along and perpendicular to the no-feathering axis, and l is the distance of the c.g. ahead of the no-feathering axis.

As the c.g. is moved, but the speed and r.p.m. are held constant: the fuselage moment will differ because of the new angle of attack; the H force will vary because of changes of attitude and cyclic control; l will change; but h will not be sensibly different, and, to maintain steady flight, T must remain practically equal to the weight. The changes in these quantities are related by the above equation as follows, then:

$$\frac{\partial M_f}{\partial \alpha_s} \Delta \phi_s = -h \Delta H + W \Delta l$$

where, since level flight was maintained, the change in fuselage angle of attack can be replaced by the change in its pitch angle.

Dividing through by Wh , there is obtained

$$\frac{1}{Wh} \frac{\partial M_f}{\partial \alpha_s} \Delta \phi_s = -\frac{\Delta H}{W} + \frac{\Delta l}{h}$$

The H force increment may be expressed as

$$\frac{\Delta H}{W} = \frac{1}{W} \frac{\partial H}{\partial a_1} \Delta a_1 + \frac{1}{W} \frac{\partial H}{\partial \alpha} \Delta \alpha$$

or, in terms of angles measured to the shaft,

$$\begin{aligned} \frac{\Delta H}{W} = & \frac{1}{W} \frac{\partial H}{\partial a_1} \Delta a_{1s} + \frac{1}{W} \frac{\partial H}{\partial \alpha} \Delta \phi_s \\ & + \left(\frac{1}{W} \frac{\partial H}{\partial a_1} - \frac{1}{W} \frac{\partial H}{\partial \alpha} \right) \Delta B_{1s} \end{aligned}$$

by converting also the c.g. position, l , to the shaft reference

$$l = l_s + h B_{1s}$$

and

$$\Delta l = \Delta l_s + h \Delta B_{1s}$$

and substituting, there is obtained

$$(7) \quad \frac{1}{Wh} \frac{\partial M_f}{\partial \alpha_s} = \frac{1}{\frac{d\phi_s}{d l_s/h}} \left\{ 1 + \frac{dB_{1s}}{d l_s/h} \left(1 + \frac{1}{W} \frac{\partial H}{\partial \alpha} - \frac{1}{W} \frac{\partial H}{\partial a_1} \right) \right. \\ \left. - \frac{1}{W} \frac{\partial H}{\partial \alpha} \frac{d\phi_s}{d l_s/h} - \frac{1}{W} \frac{\partial H}{\partial a_1} \frac{da_{1s}}{d l_s/h} \right\}$$

In this equation, the derivatives of ϕ_s , β_s , and α_s , with respect to c.g. position, l_s/h , are evaluated by taking slopes of the curves of Figure 2. The H force derivatives are calculated by equations (6d) and (6e).

As the forward speed is changed, keeping other things constant, the fuselage moment change will consist of two parts: one due to change in angle of attack, the other due to the speed change. This is expressed by

$$\frac{\partial M_f}{\partial \alpha_s} \Delta \phi_s + \frac{\partial M_f}{\partial u/U_0} \frac{\Delta u}{U_0} = -h \Delta H + W \Delta l$$

Similar changes in reference axes give the following

$$(7a) \quad \frac{1}{Wh} \frac{\partial M_f}{\partial u/U_0} = \left(1 + \frac{1}{W} \frac{\partial H}{\partial \alpha} - \frac{1}{W} \frac{\partial H}{\partial \alpha_s} \right) \frac{d\beta_s}{d u/U_0} - \left(\frac{1}{W} \frac{\partial H}{\partial \alpha} + \frac{1}{Wh} \frac{\partial M_f}{\partial \alpha_s} \right) \frac{d\phi_s}{d u/U_0} - \frac{1}{N} \frac{\partial H}{\partial \alpha} \frac{d\alpha_s}{d u/U_0} - \frac{1}{W} \frac{\partial H}{\partial u/U_0}$$

Again, derivatives of β_s , ϕ_s , and α_s , with respect to forward speed, u/U_0 , are evaluated by measuring slopes of the curves of Figure 1, and the $\frac{1}{Wh} \frac{\partial M_f}{\partial \alpha_s}$ term is known from (7). The $\frac{1}{W} \frac{\partial H}{\partial u/U_0}$ derivative need not even be calculated, since when (7a) is substituted in (3a), where it is needed, the term exactly cancels out.

The equilibrium of forces in the wind direction gives

$$D_f = -T\phi - H$$

As the c.g. is shifted, keeping speed constant and level flight,

$$\frac{1}{W} \frac{\partial D_f}{\partial \alpha_s} \Delta \phi_s = -\Delta \phi - \frac{\Delta H}{W}$$

which, upon shifting reference axes and combining with the moment relation, gives

$$(7b) \quad \frac{1}{W} \frac{\partial D_f}{\partial \alpha_s} = \frac{1}{Wh} \frac{\partial M_f}{\partial \alpha_s} - 1 - \frac{1}{\frac{d\phi_s}{d l_s/h}}$$

As speed is changed, the drag is affected by both the angle of attack and speed changes, so that

$$\frac{\partial D_f}{\partial \alpha_s} \Delta \phi_s + \frac{\partial D_f}{\partial u/U_0} \frac{\Delta u}{U_0} = -W \Delta \phi - \Delta H$$

This may be combined with the moment change for the same case to give

$$\left(1 + \frac{1}{W} \frac{\partial D_f}{\partial \alpha_s} - \frac{1}{Wh} \frac{\partial M_f}{\partial \alpha_s} \right) \frac{d\phi_s}{d u/U_0} = \frac{1}{Wh} \frac{\partial M_f}{\partial u/U_0} - \frac{1}{W} \frac{\partial D_f}{\partial u/U_0}$$

Combining this in turn with equation (7b) yields

$$(7c) \quad \frac{1}{W} \frac{\partial D_f}{\partial u/U_0} = \frac{1}{Wh} \frac{\partial M_f}{\partial u/U_0} + \frac{\frac{d\phi_s}{d u/U_0}}{\frac{d\phi_s}{d \alpha_s/h}}$$

The derivatives of fuselage pitch, ϕ_s , with respect to speed and c.g. position are taken with c.g. position and speed held constant respectively. They have been previously evaluated for use in (7) and (7a), and $\frac{1}{Wh} \frac{\partial M_f}{\partial u/U_0}$

is known from (7a). It may again be noted that the value of

$\frac{1}{W} \frac{\partial H}{\partial u/U_0}$ in (7a) appears in (7c), but that it cancels out when finally substituted into equation (1a).

Equations (6) and (7) provide the means used in this investigation for estimating the derivatives appearing in the equations of motion, (1 through 5).

B. The Analogue Computations

Considerable useful information about the natural motions defined by equations (1) through (5) can be obtained relatively easily by setting the determinant of their coefficients to zero, and solving the resulting characteristic equation. It is of sixth order, the roots typically constituting three complex pairs, indicating three modes of oscillation.

There is a very heavily damped, high frequency mode that for most purposes is probably of little interest. A short-period mode, that is roughly equivalent to the airplane's short-period mode, exists; and the long-period mode may be likened to the airplane's phugoid. The latter has received the major attention here, since the emphasis in the testing was directed in this direction, and since most of the fundamental assumptions involved in the theory seemed more applicable to slow motions. Correlation of theoretical and observed long-period motions, however, is difficult because of the

practical impossibility of recording the helicopter response for sufficiently long periods without disturbances from gusts and other random sources.

A number of solutions of the characteristic equation were made, to correlate the observed and predicted period and damping of the long-period mode. These mostly involved simplifications to the characteristic equation, as described in References 2 and 5, in order to simplify the computations. It was partly the desire to remove these approximations, and to make feasible a large number of arbitrary changes in the derivatives, that led to setting up the complete five equations on an analogue computer.

More important, however, was the desire to examine and correlate the entire transient control responses, rather than just the long-period frequency and damping. The latter alone are hardly sufficient to give a good feel for the adequacy of the theory for predicting the helicopter's handling qualities.

The control movements used in the test program were approximately rectangular pulses of the cyclic stick. The analogue computer solutions were for exactly rectangular stick movements, with amplitude and duration chosen to simulate closely the actual control motions recorded during the tests. Comparisons of computed and observed responses are shown in Figures 3 through 11. They are discussed in detail under Results and Discussion.

C. Simplified Equations of Motion

Although equations (1) through (5) can be readily solved on an analogue computer, the labor of hand solution, especially for the transient pulse responses, is quite excessive. Since analogue computers are still relatively uncommon, it is desirable to investigate the possibilities for simplifying the equations of motion without affecting too drastically the calculated responses.

The analogue computer proved an ideal tool for this investigation, too, and the various stages of simplification are indicated below.

1. The first set of simplifications corresponded roughly to those described on p.32 of Ref. 2. The neglect of gyroscopic lag of the rotor plane and the stabilizer bar permits equations (4) and (5) to be solved for a_{1s} and n_{1s} , respectively. Substitution then in equations (1), (2), and (3), reduces the number of variables and equations to three.

It is now advantageous to replace the drag equation by the combination of the drag and moment equations. The resulting three equations have the determinant given as equation (46), Reference 2. Additional assumptions that

$$s C_g L_{\alpha} \ll \frac{U_0}{g}$$

$$s C_g (D_{\alpha} - M_{\alpha r}) \doteq 0$$

$$(M_{\alpha r} + M_{\alpha_1} a_{1\alpha}) \ll 1$$

reduce the equations to the simple form

$$(8) \quad \left[\frac{U_0}{g} d + (D_u - M_u) \right] \frac{u}{U_0} + [D_\alpha - M_\alpha] \alpha_s + \left[\frac{I}{Wh} d^2 + 1 \right] \phi = 0$$

$$(8a) \quad L_u \frac{u}{U_0} + \left[\frac{U_0}{g} d + L_\alpha \right] \alpha_s - \frac{U_0}{g} d \phi = L_\alpha u_{1s}$$

$$(8b) \quad \bar{M}_u \frac{u}{U_0} + \bar{M}_\alpha \alpha_s - \left[\frac{I}{Wh} d^2 + (M_z, R_g + s C_g) d \right] \phi = u_{1s}$$

Trial solutions of equations (8) yielded results that were inappreciably different from the complete solutions, as discussed later in more detail.

2. It was further suspected that the $(D_u - M_u)$ and $(D_\alpha - M_\alpha)$ terms in (8) were insignificant, and that the lift due to control movement, $L_\alpha u_{1s}$, might be unimportant. These terms were then discarded for the final simplified case investigated:

$$(9) \quad \frac{U_0}{g} d \frac{u}{U_0} + \left[\frac{I}{Wh} d^2 + 1 \right] \phi = 0$$

$$(9a) \quad L_u \frac{u}{U_0} + \left[\frac{U_0}{g} d + L_\alpha \right] \alpha_s - \frac{U_0}{g} d \phi = 0$$

$$(9b) \quad \bar{M}_u \frac{u}{U_0} + \bar{M}_\alpha \alpha_s - \left[\frac{I}{Wh} d^2 + R d \right] \phi = u_{1s}$$

where

$$\bar{M}_u = M_u + M_{a_1} a_{1u}$$

$$\bar{M}_\alpha = M_\alpha + M_{a_1} a_{1\alpha}$$

$$R = R_g M_{a_1} + s C_g$$

Even these drastically reduced equations were found to result in but little sacrifice of accuracy, and it was felt justifiable to use them for the calculation of the helicopter's frequency response to longitudinal control, as given next section.

D. Frequency Response

The helicopter's steady-state response to sinusoidal longitudinal control movements of different frequencies was initially thought to be calculable on the analogue computer, using the complete equations of motion. This would, indeed, have been desirable, but the weak damping of the long-period mode gave trouble when this method was attempted. The starting transients took so long to die out, before leaving only the pure steady-state solution, that the method was considered impractical.

Although it would have been equally impractical in the time allowed to calculate by hand the frequency response by the complete equations, the shortened equations (9) could be handled fairly easily, and it was felt that the additional approximations involved had been justified on the basis of the analogue studies of the transient pulse responses.

The frequency responses were calculated in the standard way, using equations (9), by replacing therein the operator "d" by $i\omega$, and solving for the velocity and pitch responses, u/U_0 and ϕ , for several different frequencies. The resulting equations, left for simplicity in the complex form are

$$(10) \quad \frac{u}{U_0} = \frac{(C_u - \omega^2 C_{2u}) + i\omega (C_{1u} - \omega^2 C_{3u})}{(C_0 - \omega^2 C_2 + \omega^4 C_4) + i\omega (C_1 - \omega^2 C_3)} u_{1s}$$

where

$$(10a) \quad C_{3u} = \frac{U_0 I}{g Wh}$$

$$(10b) \quad C_{2u} = L_{\alpha} \frac{I}{Wh}$$

$$(10c) \quad C_{1u} = \frac{U_0}{J}$$

$$(10d) \quad C_u = L_{\alpha}$$

$$(10e) \quad C_4 = \left(\frac{U_0}{g}\right)^2 \frac{I}{Wh}$$

$$(10f) \quad C_3 = R \left(\frac{U_0}{g}\right)^2 + \frac{U_0}{y} \frac{I}{Wh} (L_\alpha + \bar{M}_u)$$

$$(10g) \quad C_{2\phi} = \frac{U_0}{g} (RL_\alpha - \bar{M}_\alpha \frac{U_0}{g}) + \frac{I}{Wh} (\bar{M}_u L_\alpha - L_u \bar{M}_\alpha)$$

$$(10h) \quad C_1 = \frac{U_0}{g} \bar{M}_u$$

$$(10i) \quad C_0 = L_\alpha \bar{M}_u - L_u \bar{M}_\alpha$$

$$(11) \quad \phi = \frac{-\omega^2 C_{2\phi} + i\omega C_{1\phi}}{(C_0 - \omega^2 C_2 + \omega^4 C_4) + i\omega (C_1 - \omega^2 C_3)} u_{13}$$

where

$$(11a) \quad C_{2\phi} = -\left(\frac{U_0}{g}\right)^2$$

$$(11b) \quad C_{1\phi} = -\frac{U_0}{g} L_\alpha$$

The results of these calculations are plotted in Figures 12 through 15, converted to actual speed change in m.p.h. and pitch angle in degrees, per degree of longitudinal control. For convenience in covering the wide range of values encountered, logarithmic scales are used for the plots.

Some discussion of the probable accuracy of these results, and a comparison with the frequency response of Reference 2, which was obtained by harmonic analysis of a test transient response, is given in the next section.

V. RESULTS AND DISCUSSION

At the outset of a presentation of results, and a discussion of their meaning, it is desirable to clearly define the purpose of the study, in order not to become lost in details not pertinent to the main objectives. The principle objective of this work was to answer, if possible, the following two questions:

- (1) Are the equations theoretically derived capable, even with complete freedom to choose values for the derivatives, of predicting, with reasonable accuracy, the longitudinal control response of the helicopter; and if so,
- (2) Are the required values of the derivatives reasonable, in that they agree with values obtained by some other independent method, such as theory, wind-tunnel, or steady-state flight data?

Although the indications are that the answers to these are affirmative, they can not go entirely unqualified. The data are not sufficiently self-consistent to permit a completely positive answer to question (1), and the alternate sources of information on the required derivatives are in some cases sufficiently dubious that an unqualified answer to (2) is impossible. These points are discussed in more detail in the following pages.

A. The Transient Pulse Responses

The analogue computer solutions for the helicopter transient response to longitudinal control pulses are compared with the recorded flight data in Figures 3 through 11. Quantitative agreement between them is limited principally by the following three factors:

1. The observed test transients were in some cases unquestionably affected by gusts, for which there is no way to allow in the computations. This factor is readily apparent, for example, in Figure 11, where there is no other apparent explanation of the fact that the steady-state of the airspeed response is displaced from zero; and in Figure 6, where the apparent sudden shortening of period at about twelve seconds is difficult to explain in any other way.
2. The failure, or inability, of the pilot to return the longitudinal control to zero, and to hold it steady, after application of the pulse disturbance. This difficulty is exemplified by Figures 3, 4, 5, 8, and 9, where considerable of the disagreement between computed and observed responses is traceable to this effect.
3. Discrepancies between the shapes of pulses used in the tests and on the analogue computer cause differences in the responses, particularly in the first few seconds of response where the frequency content of the input in the short-period range is of importance. It was not possible, of course, for the pilot to move

the control instantaneously; nor was it feasible, with the analogue equipment available, to simulate exactly the shape of control movement recorded in the tests. The best practical solution was to use, in the computation, rectangular pulses matching approximately the test pulses in area and duration. The result, of course, is that all the computed responses are too fast, and have somewhat too great an amplitude, in the first few seconds. The effect on the long-period response, at times greater than about eight seconds, would be expected to be generally negligible.

Detailed discussion of the individual transients is given later in this section. It is felt that, in view of the above three difficulties, the computed and observed transients are in satisfactory agreement; and that in answer to question (1) above, it should be stated that the equations of motion given earlier are capable of predicting, with reasonable accuracy, the helicopter control response.

B. The Stability Derivatives

The rationality of the stability derivatives used to obtain the computed responses shown in Figures 3 through 11 is, of course, a question of great interest.

It had been suspected, from the work in Reference 2, where only the period and damping of the long-period mode were considered, that the only really important stability derivatives are the static stabilities M_u and M_α ; the lift derivatives, L_u and L_α ; and the bar and rotor gyroscopic coefficients, C_g and R_g . It had been verified there that, at least as far as the roots of the characteristic equation are concerned, equations (48), (49), and (50), (of Reference 2), in which all other derivatives are neglected, yielded results in satisfactory agreement with the more complete equations. It has been shown in this study, that the other derivatives can also be neglected, for practical purposes, in calculating the transient responses. For the responses of Figures 3 and 5, for example, analogue computations using equations (9) gave results at no times more than 15% different from those shown in the figures, which were calculated by the more complex equations (1) through (5). Discrepancies in the long-period mode of response were especially negligible, with even the 15% errors limited to the first few moments of response.

Since it is fundamentally impossible to obtain information about derivatives which do not materially influence the recorded data, it is not possible, for example, to evaluate the reliability of equations (7b) and (7c), for the drag derivatives, by comparing calculated and observed transients. For this reason, the discussion below, of the derivatives used, is limited to those which are important to the motions.

The fuselage stabilities, M_{uf} and M_{α_f} , have been evaluated by equations (7) and (7a); for the case of normal damper setting, normal c.g. position, and 333 rpm; over the speed range from 20 to 80 mph. The curves of trim at various speeds and c.g. positions are shown as Figures 1 and 2. The derivatives of cyclic control, fuselage pitch, and flapping, as required in equations (7) and (7a), are determined as the slopes of these curves.

Some scatter is evident in this data. It is believed, however, that there are sufficient points that the curves are fairly well established, and that the resulting values of M_{u_f} and M_{α_f} are reasonably accurate.

Values of these two fuselage stability derivatives, obtained by the method of equations (7) and (7a) are shown below. The damper setting was normal, the c.g. position intermediate, and the rpm was 333.

Speed, mph	20	40	60	80
M_{α_f}	-.200	-.239	-.220	-.239
M_{u_f}	-.035	-.024	+0.007	+0.071

The large negative (stable) values for the angle-of-attack stability are significant, in that they differ drastically from theoretical predictions (see Reference 2). The theory, however, included the effects of rotor downwash only in a very approximate fashion. It was further shown in Reference 2, and entirely verified in the analogue computer studies here, that only a large, stable, M_{α} can account for the stability of the long-period mode of the helicopter's dynamic response characteristics. It is therefore concluded that the values for M_{α_f} given above are reasonably close to the truth. It can only be assumed that the difficulty of explaining them on theoretical grounds is due to very complicated rotor downwash effects.

The contributions of the rotor to the M_{α} derivative are minor compared to the large fuselage effects given above. For example, at 60 mph, the direct rotor contribution calculated by the last two terms of equation (3b) is

$$M_{\alpha_r} = -.025$$

and the contribution due to change in flapping is

$$M_{\alpha, a_{1\alpha}} = +0.033$$

The calculated rotor effects on M_{α} are thus small, and tend to cancel. It seems unlikely that even large percentage errors in estimating these would be of any importance in this case.

The values for the fuselage speed stability, tabulated above, as obtained from the steady-state data, are somewhat more questionable, since the method of calculating them is not so direct as for the M_{α} derivatives. Also, the curves drawn with $\frac{u}{U_0}$ as independent variable are more difficult to fair (Figure 1), and the slopes are less likely to be accurate.

The rotor contributions are here relatively more important, so that errors in their estimation would be more significant. The various contributions are compared below.

SPEED , mph.	20	40	60	80.
M_{u_f}	-.035	-.024	+.007	+.071
M_{u_r}	+.018	+.010	+.013	+.022
$M_{a, a_{1u}}$	+.015	+.026	+.035	+.042
\bar{M}_u	-.002	+.012	+.055	+.135
$\bar{M}_{u emp.}$	-.002	+.056	+.089	+.186

The values tabulated in the fourth row are the sums of the first three rows, and represent estimated total static speed stability. The last row shows the empirical values used in the analogue computations to obtain the agreement on transient responses shown in Figures 3 through 11. The empirical values were determined primarily by the necessity of making the periods of the long-period mode agree with those observed. The frequency of the natural oscillation is very sensitive to \bar{M}_u , so that the values given in the last row are probably close to being correct.

While the discrepancies shown are large enough to be of interest, they are not too large to explain by possible errors in the theoretical estimates of the rotor contributions, or by cumulative errors in the determination of the fuselage part.

The trend of rapidly increasing fuselage stability with forward speed, is, of course, very important, and is unmistakably verified by comparing the first and last rows of the table. It may also be pointed out that this trend, toward greater fuselage speed stability with increasing speed, should be expected only for a fuselage statically stable with angle of attack. This is because positive speed stability is associable with nose-up trim moments, and the latter will increase with speed because of the more nose-down angle of attack only if the fuselage is statically stable ($M_{\alpha_f} < 0$). This trend constitutes therefore an additional confirmation of the large negative values of M_{α_f} previously discussed.

The lift derivatives, with respect to angle of attack and speed, were assumed to be independent of the fuselage and to consist only of the rotor contributions. The values of these, calculated by equations (6) and (6a) are compared below with the empirical values required for the agreement shown in Figures 3 through 11. Again, the c.g. was in its "normal" position, the damper setting was normal, and the rpm was 333.

SPEED , mph.	20	40	60	80
$L_{u\ est.}$	+0.320	+0.157	+0.009	-0.121
$L_{u\ emp.}$	+0.025	+0.019	+0.009	-0.121
$L_{\alpha\ est.}$.62	1.40	2.31	3.07
$L_{\alpha\ emp.}$.10	.38	1.43	3.07

It is seen immediately from the table that at the high speed the theoretical values are satisfactory. As the speed is reduced, the agreement is poorer, until at the lowest speeds, the theoretical values are entirely inadequate.

It is to be expected that the disagreements should be more pronounced at low speed, since the effects of induced velocity changes with speed and angle of attack are there more important and more unpredictable. For example, if the $L_u = .320$ in the 20 mph case had been calculated assuming that the induced flow did not change with forward speed; instead of by equation (6), where it was assumed always given by (21) of Reference 2; the value would have been negative, and of about the same magnitude. Since which is the better assumption is a debatable point, it is not too surprising to find the empirical value about midway between the two extremes.

It is really disappointing that the values of L_{α} are not in better agreement, since that derivative should be the most easily predictable of all. Again, the agreement is good at high speed, but very poor at low speed, where the induced velocity effects are uncertain.

The empirical values of L_u and L_{α} were primarily determined by their effects on the amplitude of the transient responses. L_{α} affects in a particularly noticeable way the relative excitation of the long and short period modes, while L_u is important to the relative excitation of the velocity and pitch responses. While great accuracy can not be claimed for the empirical values tabulated in view of the somewhat imperfect correlation of transients, it is believed that the indicated trends are correct, and that the large disagreement with theory, at low speeds, is significant.

The rotor and bar gyroscopic coefficients, R_g and C_g were calculated according to the theoretical equations (4c) and (5a). There was no sound basis for arbitrarily modifying them, and it proved impossible to improve the correlation of the transient responses appreciably by assuming different values.

In particular, it was verified on the analogue computer that even large increases in C_g would not predict the stable phugoid mode, un-

less M_{α} were stable. The principal effects of very large C_g , not apparent in the observed responses would be: (1), strong tendency to destabilize the short-period mode; (2) reduction of the amplitude of response for given input; and (3), lengthening of the period of the phugoid mode.

Limited direct analysis of the data for bar deflection vs pitch rate indicated the effective C_g to be about the theoretical value. This was limited by the accuracy of the recorded bar deflection data, which was poor, and by the fact that, in the absence of direct pitch rate measurements, the pitching velocity had to be found from the slope of the pitch angle curves.

The available evidence thus suggests that the theoretical bar and rotor coefficients are satisfactorily accurate; at least, in the case of the bar, for the normal damper setting.

C. Bar Damper Setting

The effects of changing the bar damper setting, observed in the recorded transients, can be assessed by comparing Figures 9 through 11. It had been assumed, by analogy with the hovering case, that loosening the bar dampers would stabilize the long-period mode of response; and the data (principally the pitch responses) were originally interpreted as verifying this prediction. Re-examination of the data (particularly with more weight given to the velocity response) forced the conclusion that this was incorrect. The apparent effects of loosening the dampers are: (1), to drastically reduce the excitation of the long-period mode, especially the pitch response, without affecting in proportion the short-period excitation; (2), to increase the period of the phugoid mode; (3), to change the damping of the phugoid mode, as evident in the velocity responses, an inappreciable amount. It is very easily understood, incidentally, how pilots could misinterpret the reduction of excitation of a marginally stable mode as increased stability.

Points (2) and (3), above, are in agreement with the theoretical predictions previously discussed. The point of discrepancy is, however, that whereas the theory indicates approximately proportional reduction of the entire responses due to increasing C_g , the data shows a super-proportional reduction of the pitch response in the phugoid mode. If, in the analogue computations shown in Figure 11, for the loose damper setting, C_g were taken large enough to give good agreement on the long-period pitch response, then the initial, short-period, response would be far too small, and the short-period mode would show very light damping. The latter, incidentally, was never noticed by the pilot, as it should have been if actually present; nor was it observed in the reduction of the test data.

The only way, within the framework of the present theory, to resolve this discrepancy, is to allow the lift derivative, L_{α} , to vary with damper setting. As previously noted, L_{α} affects the relative excitation of short and long period modes. In the computed transients, Figures 9 through 11, this variation was allowed, in order to obtain even the qualitative agreement shown. The values of all derivatives were held constant, except C_g and L_{α} , which are tabulated below:

DAMPER SETTING:	1 (hard)	2 (normal)	3 (soft)	4
C_q	.10	.17	.22	.33
L_{ω}	5.70	1.43	1.00	.28

Since any effect of damper setting on L_{ω} is physically difficult, if not impossible, to understand, no real significance is attached to this result.

It was thought that coupling in the bar between lateral and longitudinal modes might possibly account for the discrepancies, so the study given in the Appendix was carried out. The result, however, indicated the approximate bar equation (5) to be adequate, and showed that such lateral coupling would be negligible.

It is assumed that the disagreement on the effects of changing damper setting, is associated with either (or both) the feedback of blade feathering moments to the bar, or non-linearity of the bar dampers in any setting except the normal one. (See discussion, Ref. 2, p.55) It has not been feasible, in the time allotted for this investigation, to examine these possibilities in detail.

D. The Individual Transient Responses

1. 20 mph (Figure 3)

Agreement between calculated and observed responses is good. The somewhat different shape of the short-period response, noticeable in the pitch angle, is common to all the comparisons, and is readily explainable by the difference in input pulse shapes. The small excitation of the phugoid mode, relative to the short period, requires the low value of L_{ω} compared to the theoretical as previously discussed.

2. 40 mph (Figure 4)

Good agreement can not be expected here, where the differences in pulse shape and the failure to hold the control steady after the pulse are important. Judging particularly by the nature of the pitch response in the neighborhood of 6 seconds, the motion may have been influenced strongly by a gust at that time. The best that can be said is very qualitative -- that had these extraneous factors not interfered, it looks as though the agreement would be reasonable.

3. 60 mph (Figure 5)

The natures of computed and observed responses are in excellent agreement. The fact that the observed steady-state velocity response is non-zero implies that the control was not returned to the trim position, as shown. This effect is also evident in the pitch

response, where it can account for most of the discrepancies.

4. 80 mph (Figure 6)

Agreement is reasonable, up to about 12 seconds, where the motion seems to have been influenced by a series of gusts. The test data for both forward and aft c.g. locations (Figures 25e and 27e, Reference 1) both show phugoid periods in agreement with the computation, and it seems unreasonable to suppose that the apparent sudden shortening of period after 12 seconds shown in Figure 6, is due to anything except extraneous effects, such as gusts.

5. Forward c.g., 60 mph (Figure 7)

Agreement on the phugoid response is generally satisfactory. Improved correlation on the short period response in the pitch angle could be achieved by modifying the value of L_{α} used, but this would be inconsistent with the other cases.

6. Reduced rpm, 60 mph (Figure 8)

The principal discrepancy is in the steady-state values of the responses, which are non-zero clearly because the control was not returned to zero. The sluggish short-period response, while not too significant, might be associable with a slower pulse application than indicated by the data. Agreement could be improved by modifying certain derivatives, but this would again be inconsistent with other cases, where the correlation was better.

7. Hard Dampers (Figure 9)

The very large excitation of the phugoid mode is amply evident in the observed response. The agreement shown is not bad, considering the large control movements after the pulse; but it could only be obtained, as previously discussed, by the somewhat irrational use of large L_{α} .

8. Soft Dampers (Figure 10)

Again, agreement or disagreement here is probably not significant, since it was necessary to modify L_{α} arbitrarily. The effects of damper non-linearity at other than normal settings seem likely to be important. This is a difficult matter to investigate theoretically, and it has not been feasible to do so within the scope of this work.

9. Very Soft Dampers (Figure 11)

The large reduction in excitation of the phugoid mode of pitch response is especially evident. The lengthening of period is seen, particularly in the velocity response, where it is also obvious that the phugoid mode is not heavily damped. Similar observations can be made of the responses at 50 and 80 mph, Figures 30c and 30e, Reference 1. The

very small L_{α} used in the calculations seems likely not to be the correct explanation. Further increase of C_g does not give better agreement, since it reduces the amplitude of the short period response too much, and would produce a very lightly damped short-period mode, which is nowhere evident in the data.

E. Frequency Response

Equations (10) and (11) of this report were used to calculate the helicopter frequency response at different speeds, shown in Figures 12 through 15. Values of the various derivatives were the same as those used in obtaining the analogue computer transient responses previously discussed.

Surely the frequency responses shown are more accurate in the low frequency range than in the high, since the empirical method of determining the derivatives weighted the long-period mode more heavily. Also, of course, the theoretical equations used for calculations involve assumptions that are certainly not valid above, say, rotor rpm, or about 5 cycles per second. The calculations might nevertheless be useful in autopilot design, where stabilization of the phugoid mode, involving only low frequencies, would be the principal aim.

Direct comparison with test data is only possible for the 60 mph forward speed, (Figure 14), where the experimental points shown are taken from Reference 2, Figure 4. Those points were obtained by harmonic analysis of the transient response. Good accuracy, particularly in the phase data, is difficult to maintain with that technique where the amplitude of response is small, as it is above about .1 cycle per second. This is substantiated by the scatter of the points at the higher frequencies.

In spite of the difficulties of obtaining the frequency response experimentally by harmonic analysis of transients, and of the many assumptions and simplifications involved in the theory, agreement between the two is seen to be pretty good. Especially, the amplitude curves fit the data well. The only serious discrepancies are in the phases of the velocity response. Time, unfortunately, has not permitted more extensive investigation of the possible causes.

VI. CONCLUSIONS

As a result of further studies of the H-13 Helicopter transient response data, and further theoretical calculations of response characteristics, using an analogue computer, the following conclusions are drawn:

A. The equations of motion given herein, for the longitudinal dynamic response of a gyroscopically stabilized helicopter in forward flight are capable, given the proper values of the derivatives, of predicting with satisfactory accuracy the responses which were observed in flight-testing.

B. The proper values of the important derivatives would not, in general, be predicted by existing theories.

In particular,

1. The large stable contribution of the fuselage to the angle-of-attack moment derivative is verified by steady trim data, and would not have been predicted by any existing theory.

2. The stable contribution of the fuselage to the moment derivative with respect to speed changes, partially verified by analysis of steady-state data, would not have been predicted theoretically, but might be expected in combination with strong angle-of-attack stability.

3. The important lift derivatives are not given to satisfactory accuracy by any of the existing theories, especially at low forward speed, where the theoretical treatment of the downwash is doubtful.

C. For most purposes, involving interest in only the slower modes of motion, the greatly simplified equations of motion presented herein should be adequate, since comparisons with solutions of the more complete equations showed little sacrifice of accuracy. Differences due to the additional assumptions involved would be entirely overshadowed by inaccuracy in estimating the more important derivatives.

D. The simplified equations predict with reasonable accuracy the frequency response information derived from the original test data.

E. The effects of non-standard bar damper settings are still not satisfactorily explained. It is assumed that they are associated with damper non-linearities. Re-examination of the data, at least, however, confirms the prediction that loosening the dampers does not materially increase the damping of the phugoid mode. The data indicates that softening the dampers reduces the pitching excitation of the phugoid mode, giving the false impression of increased stability.

LIST OF REFERENCES

1. Gould, A; Seal, J.C.; and O'Dea, J.: "Transient Responses of an H-13 Helicopter to Longitudinal Stick Pulses as Measured in Flight", Cornell Aeronautical Laboratory Report # TB-641-F-1; 15 November 1950.
2. Seckel, E.: "Comparison Between Theoretical and Measured Longitudinal Stability Characteristics of a Gyroscopically Stabilized Helicopter in Forward Flight". Cornell Aeronautical Laboratory Report # TG-641-F-2; March 16, 1951.
3. Hohenemser, K.: "Contribution to the Problem of Helicopter Stability". Preprint for a Discourse for the Helicopter Design Session at the 4th Annual Forum of the American Helicopter Society; April 1948.
4. Speth, R. : "Analysis of 1/20 Scale Model 47 Helicopter Stability Tests in the 2 1/2' x 4' Purdue Wind Tunnel"; Bell Aircraft Corp. Report No. 47-943-002; September 17, 1946.
5. Seckel, E.: "Correlation of Some Longitudinal Dynamic Stability Characteristics of a Bell Helicopter from Theory and Flight Tests." Preprint No. 356 for Discourse at the 20th Annual Meeting of the Institute of the Aeronautical Sciences; January 1952.

APPENDIX - The Bar Equation

Because of the difficulties of explaining the effects of changing damper settings, noted in Results and Discussion, it was deemed advisable to re-examine the bar equation, (5). That equation involves the assumption (References 1 and 3) that the bar mass is concentrated in a ring, similar to a gyroscopic ring. A better approximation would surely be that the bar mass is concentrated at two points at opposite ends of a weightless rod. It was thought that this might lead to some lateral coupling, which might explain the effects of changing damper setting. It is shown below that, in fact, some lateral coupling will exist, but that for frequencies involved in the phugoid mode, the effect is negligible.

It can be shown that the instantaneous acceleration, in a vertical plane and normal to the bar, of the concentrated mass at the tip is

$$\begin{aligned} \frac{\ddot{z}}{r} = & \ddot{\eta}_s - \ddot{\phi} \cos \psi_1 + \sin \eta_s \cos \eta_s (\Omega^2 - \dot{\phi}^2 \sin^2 \psi_1) \\ & + 2 \Omega \dot{\phi} \cos^2 \eta_s \sin \psi_1 \end{aligned}$$

For small disturbances, this may be linearized to

$$\frac{\ddot{z}}{r} = \ddot{\eta}_s - \ddot{\phi} \cos \psi_1 + \Omega^2 \eta_s + 2 \Omega \dot{\phi} \sin \psi_1$$

If it be assumed that the bar motion is first harmonic, so that

$$\eta_s = -m_{1s} \cos \psi_1 - m_{1s} \sin \psi_1$$

and this relation be substituted above, then the inertia moment acting on the bar is

$$\begin{aligned} M_i = & -mr\ddot{z} = -mr^2 \frac{\ddot{z}}{r} = -I_b \frac{\ddot{z}}{r} \\ = & -I_b \left[(2\Omega \dot{m}_{1s} + 2\Omega \dot{\phi} - \ddot{m}_{1s}) \sin \psi_1 \right. \\ & \left. - (\ddot{m}_{1s} + \ddot{\phi} + 2\Omega \dot{m}_{1s}) \cos \psi_1 \right] \end{aligned}$$

The damper moment is

$$M_d = -C\dot{\eta}_s = -C \left[(\Omega n_{1s} - \dot{m}_{1s}) \sin \psi_1 - (\Omega m_{1s} + \dot{n}_{1s}) \cos \psi_1 \right]$$

If the two moments be summed and set to zero, the coefficients of $\sin \psi_1$ and $\cos \psi_1$, must independently equal zero. Thus, the two equations of bar motion are obtained:

$$(12a) \quad (C_g d + 1) n_{1s} - \left(\frac{C_g}{2\Omega} d^2 + \frac{1}{\Omega} d \right) m_{1s} = -C_g d \phi$$

$$(12b) \quad \left(\frac{C_g}{2} d^2 + d \right) n_{1s} + (\Omega C_g d + \Omega) m_{1s} = -\frac{C_g}{2} d^2 \phi$$

The solutions of these for n_{1s} and m_{1s} are

$$(13a) \quad n_{1s} = \frac{-\left(\frac{C_g}{4} d^3 + \frac{1}{2} d^2 + \Omega^2 C_g d + \Omega^2 \right) C_g d \phi}{\frac{C_g^2}{4} d^4 + C_g d^3 + (1 + \Omega^2 C_g^2) d^2 + 2\Omega^2 C_g d + \Omega^2}$$

$$(13b) \quad m_{1s} = \frac{\Omega \frac{C_g}{2} d^2 \phi}{\frac{C_g^2}{4} d^4 + C_g d^3 + (1 + \Omega^2 C_g^2) d^2 + 2\Omega^2 C_g d + \Omega^2}$$

Since $\Omega \gg 1$, $\Omega^2 C_g^2 \gg 1$, and for low frequency modes, such as the phugoid, d is small, these may be simplified to

$$(13c) \quad n_{1s} = \frac{C_g d \phi}{1 + C_g d}$$

$$(13d) \quad m_{1s} = \frac{\frac{C_g}{2\Omega} d^2 \phi}{(1 + C_g d)^2}$$

It may be noted that the expression for the longitudinal tilt is exactly equation (5). The ratio of lateral to longitudinal tilt is

$$(14) \quad \frac{m_{1s}}{n_{1s}} = \frac{1}{2\alpha} \frac{d}{1 + c_g d}$$

For the phugoid mode, neglecting damping, d may be set equal to $\frac{2\pi}{P}$ where P , the period, is of the order of 20 seconds. The ratio is approximately

$$\frac{m_{1s}}{n_{1s}} \approx .005$$

It is thus verified that for slow motions, as are involved in the phugoid, the lateral coupling is negligible, and equation (5) is suitable for the longitudinal bar motion.

It seems likely that the effects of changing damper setting, unsatisfactorily explained in the main body of the report, may be associated with non-linearity of the bar dampers.

LIST OF FIGURES

Figure No.	Description	Page No.
<u>Steady-State Trim Data:</u>		
1.	Plotted Against Forward Speed	39.
2.	Plotted Against c.g. Position	40.
<u>Comparison of Calculated and Observed Transient Responses:</u>		
3.	<u>20 mph</u> ; normal c.g., 333 rpm; normal dampers	41.
4.	<u>40 mph</u> ; normal c.g., 333 rpm; normal dampers	42.
5.	<u>60 mph</u> ; normal c.g., 333 rpm; normal dampers	43.
6.	<u>80 mph</u> ; normal c.g., 333 rpm; normal dampers	44.
7.	60 mph; <u>forward c.g.</u> , 333 rpm; normal dampers	45.
8.	60 mph; normal c.g., <u>300 rpm</u> ; normal dampers	46.
9.	60 mph; normal c.g., 333 rpm; <u>hard</u> dampers	47.
10.	60 mph; normal c.g., 333 rpm; <u>soft</u> dampers	48.
11.	60 mph; normal c.g., 333 rpm; <u>very soft</u> dampers	49.
<u>Frequency Response to Longitudinal Cyclic Control:</u>		
12.	<u>20 mph</u> ; normal c.g.; 333 rpm; normal dampers	50.
13.	<u>40 mph</u> ; normal c.g.; 333 rpm; normal dampers	52.
14.	<u>60 mph</u> ; normal c.g.; 333 rpm; normal dampers	54.
15.	<u>80 mph</u> ; normal c.g.; 333 rpm; normal dampers	56.

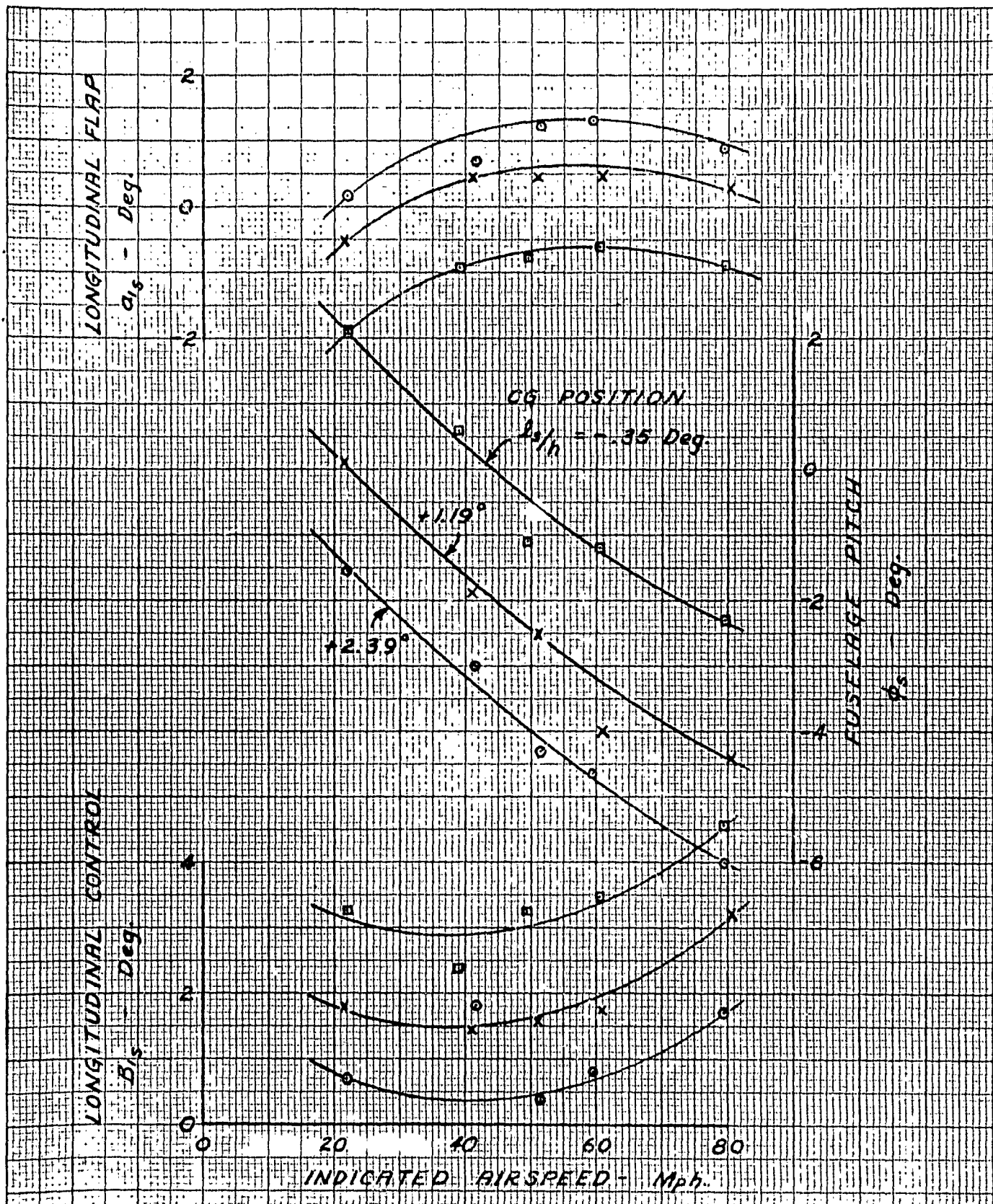
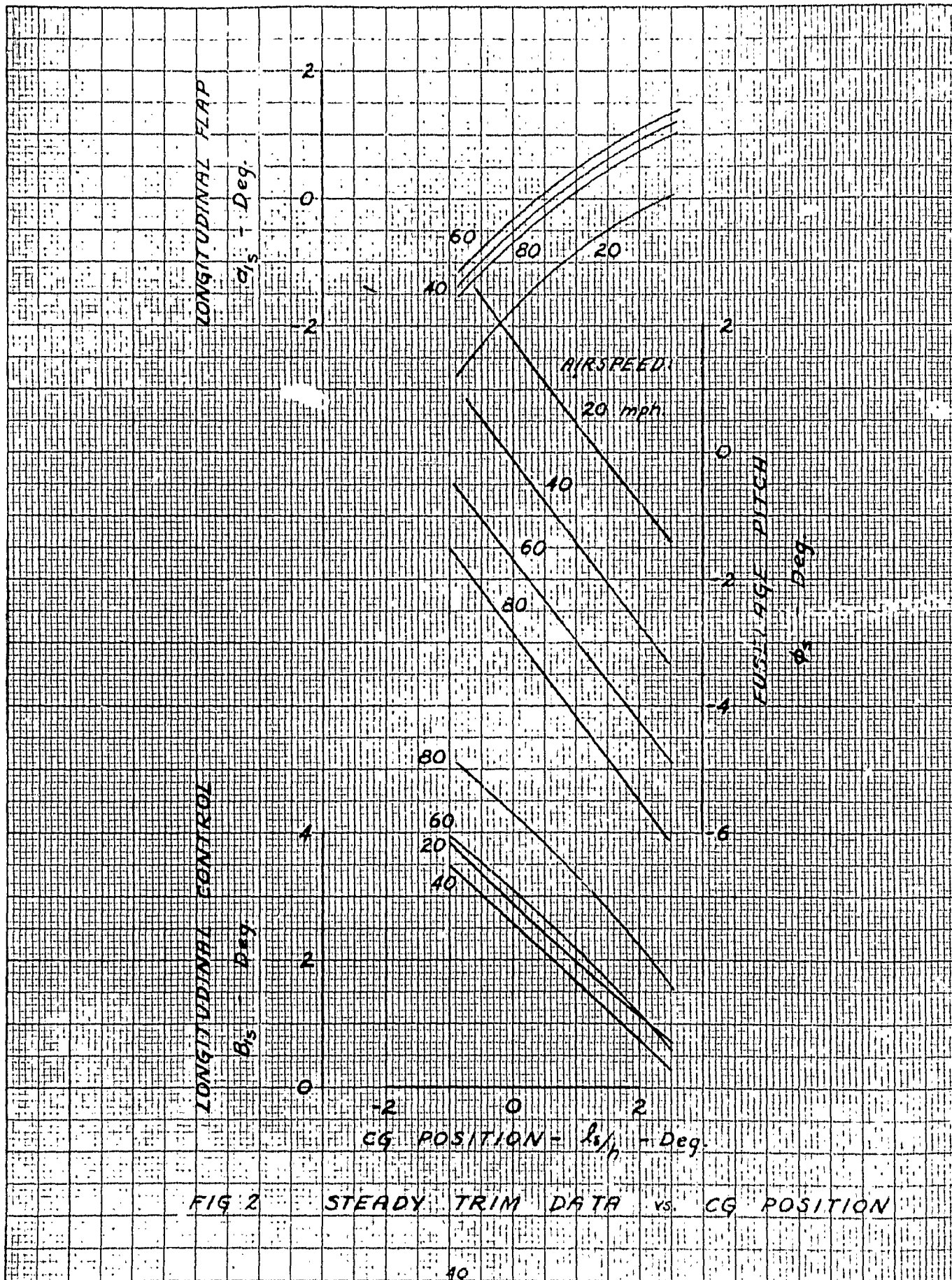


FIG 1 STEADY TRIM DATA vs. AIRSPEED



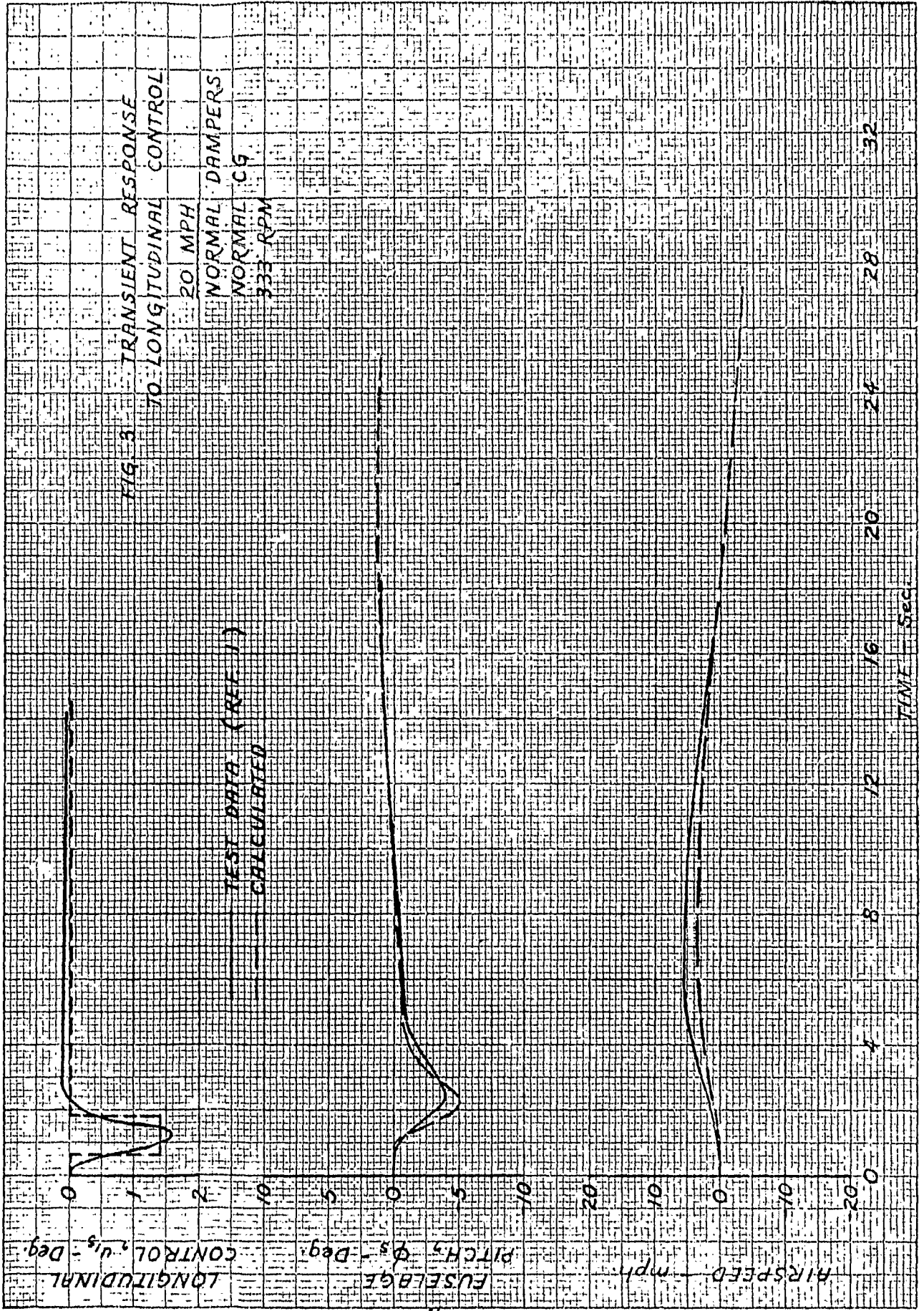
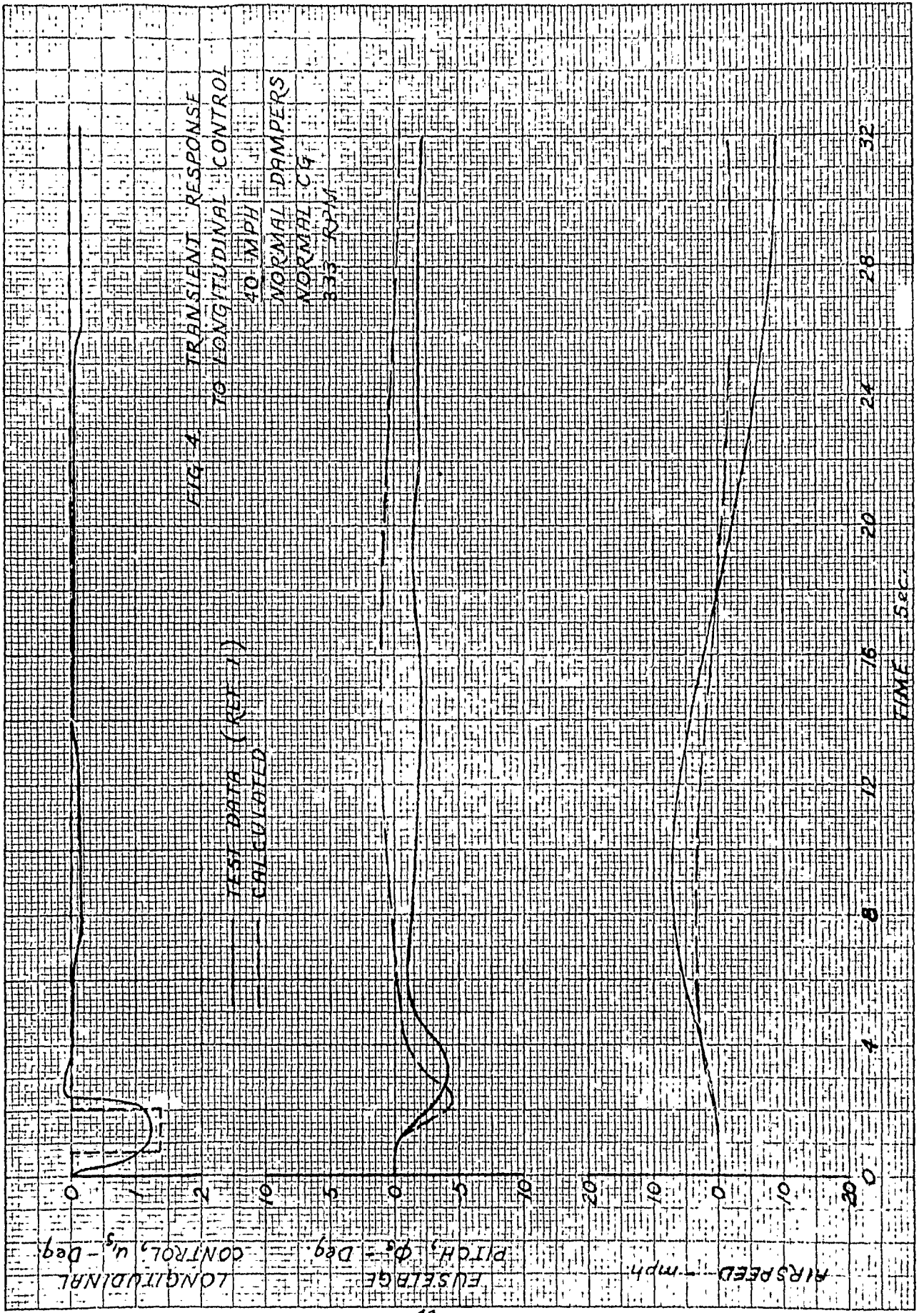


FIG. 3 TRANSIENT RESPONSE TO LONGITUDINAL CONTROL

20 MPH
NORMAL
NORMAL CG
333-RPM

0 4 8 12 16 20 24 28 32



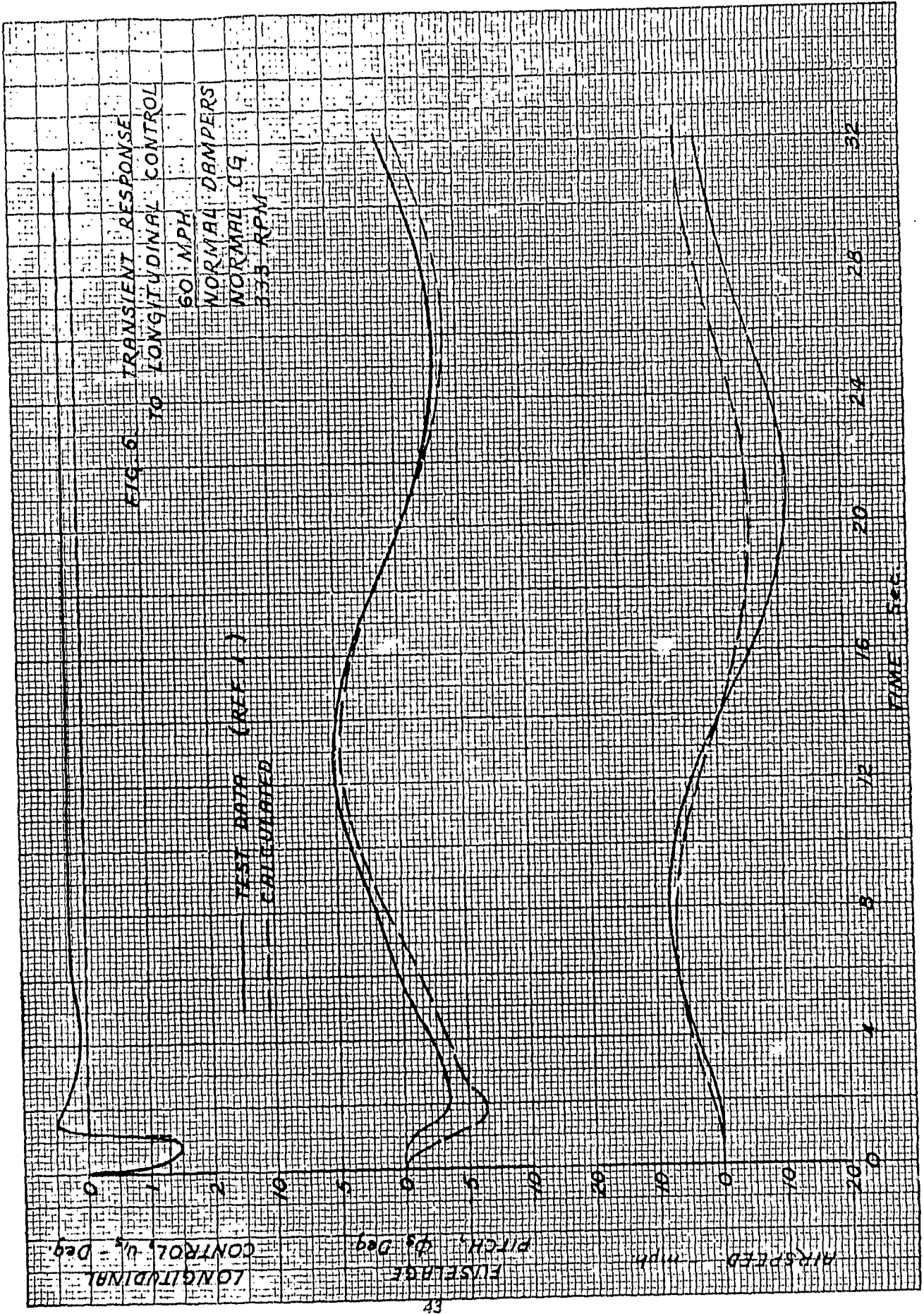


FIG. 6
 TRANSIENT RESPONSE
 TO LONGITUDINAL CONTROL
 60 MPH
 NORMAL DAMPERS
 NORMAL CG
 333 RPM

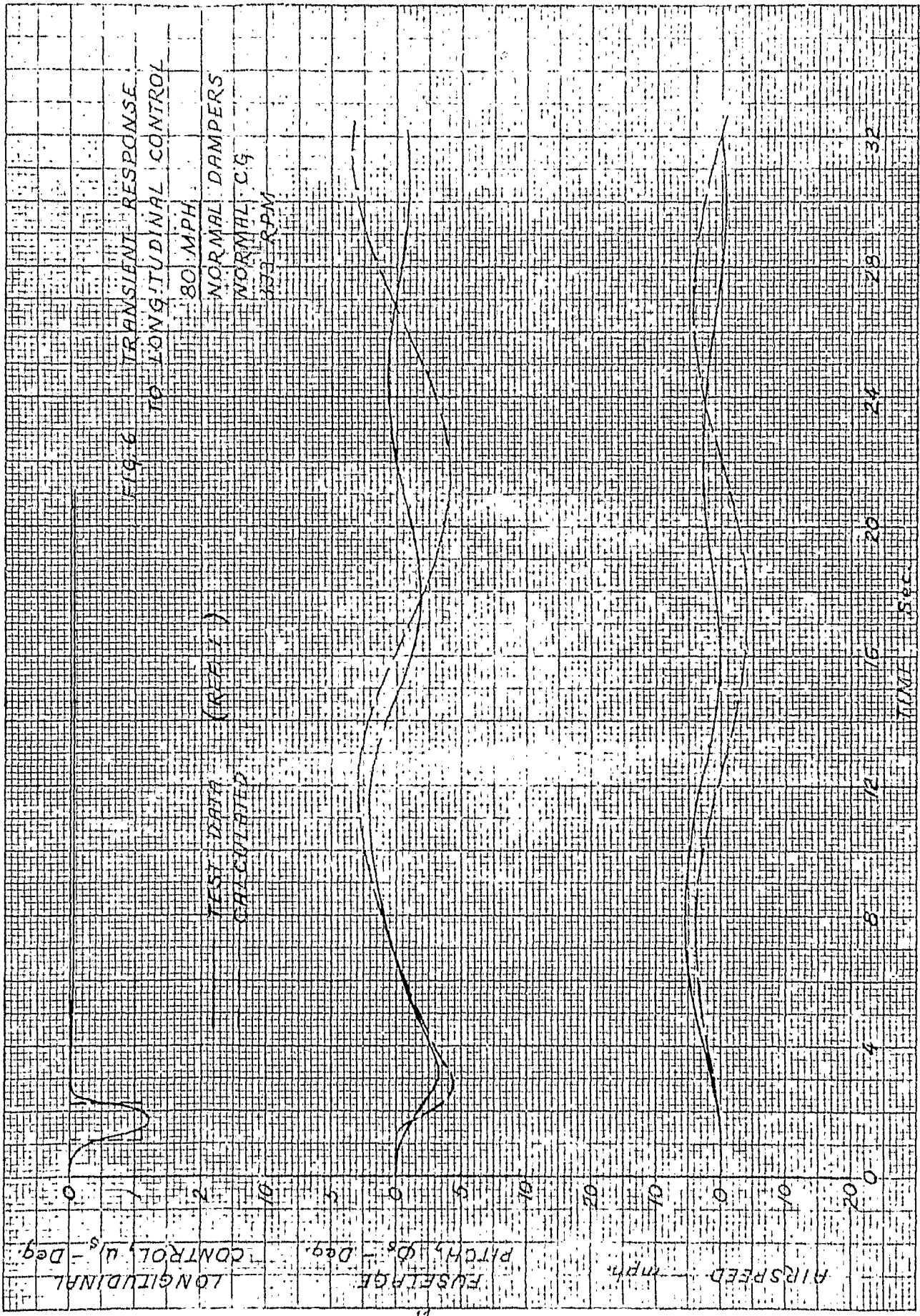
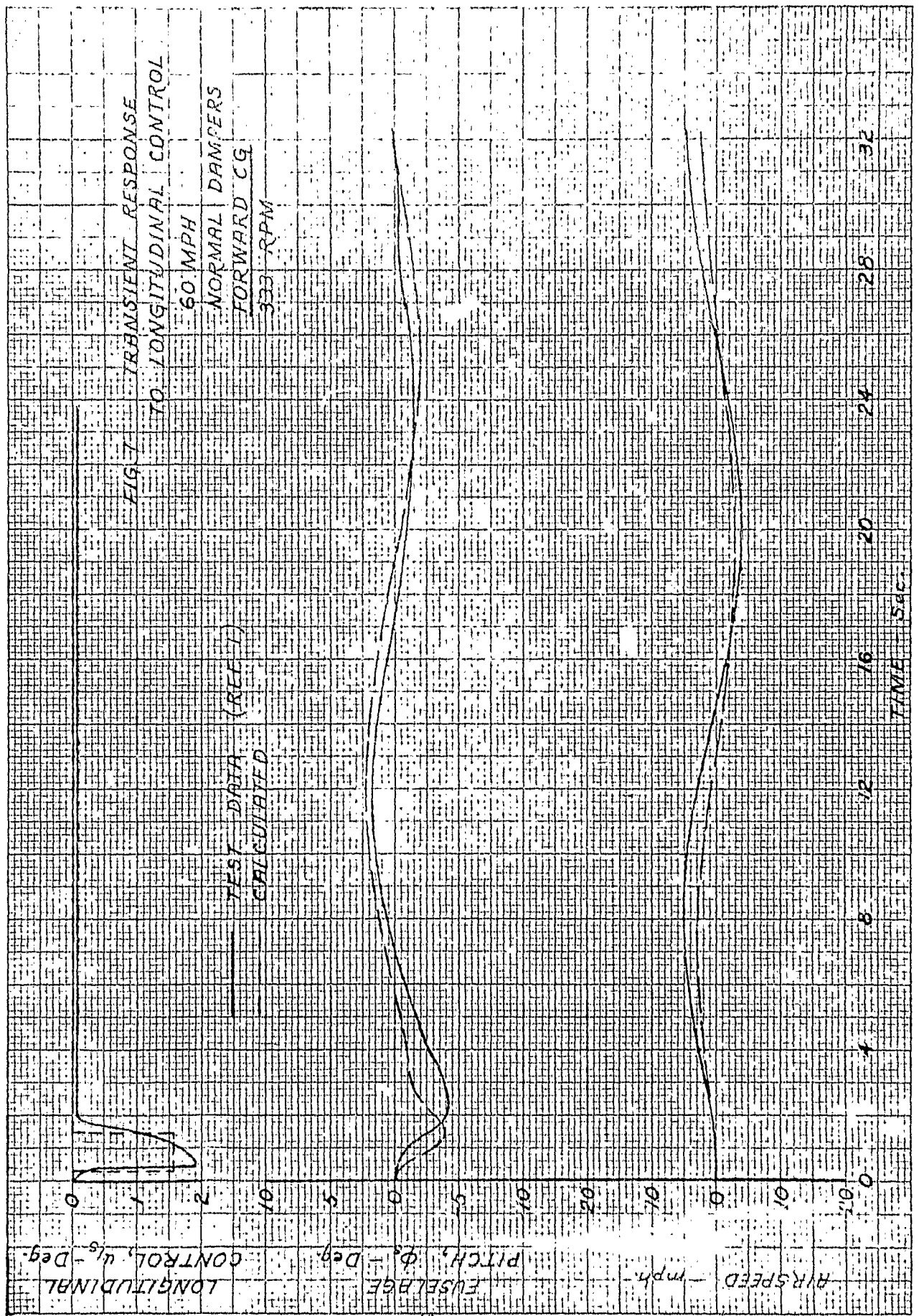
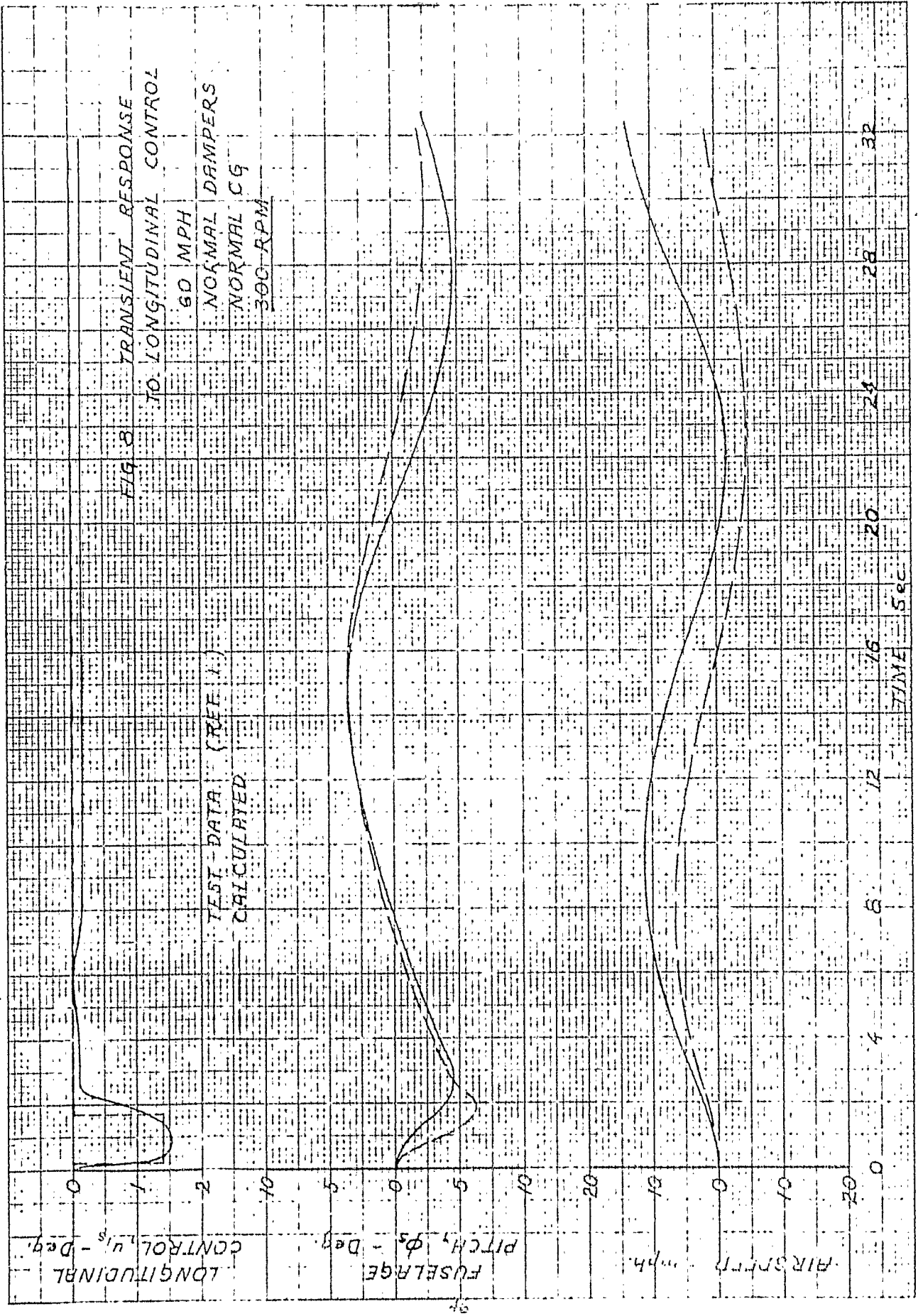
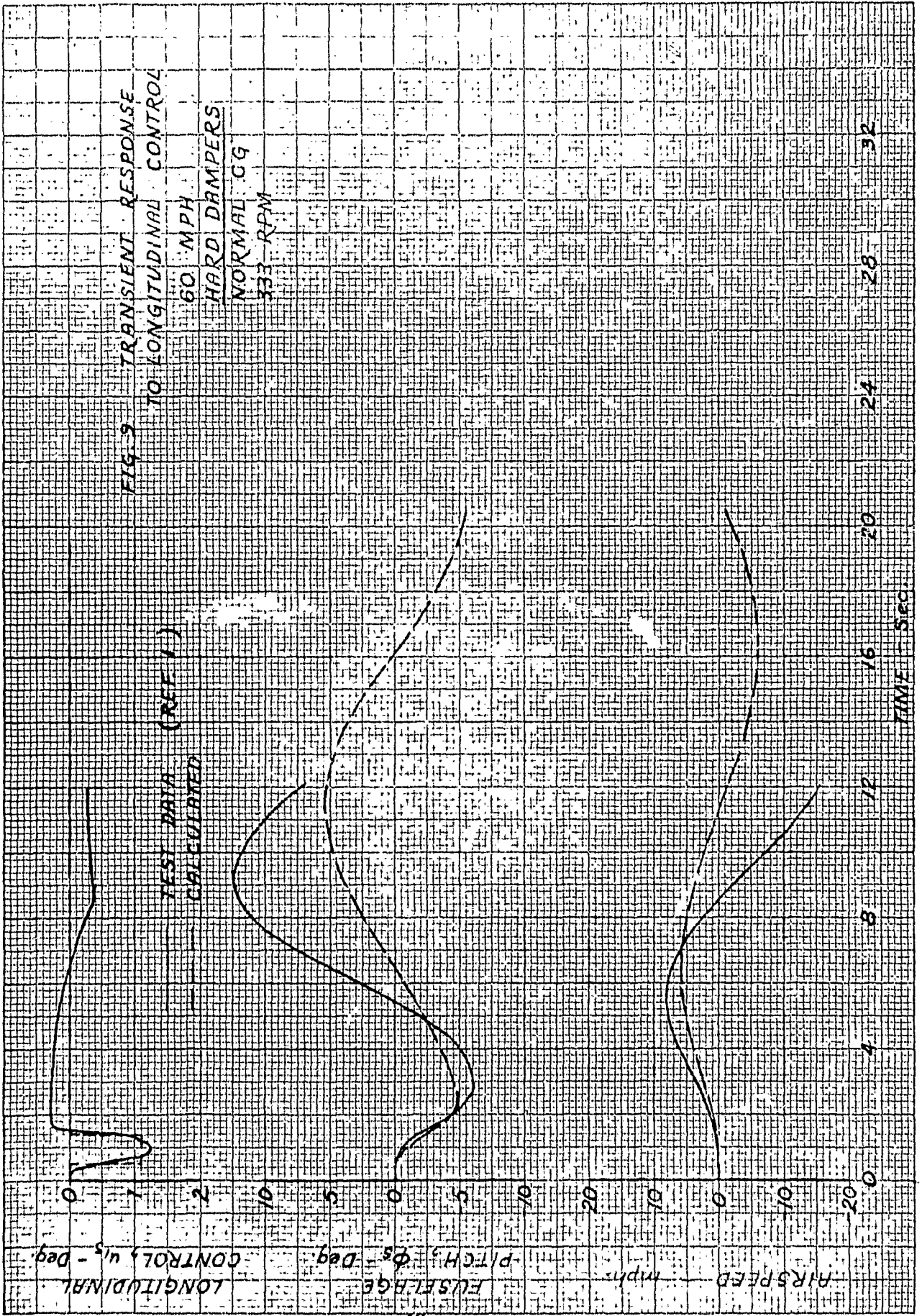


FIG. 6 TRANSIENT RESPONSE TO LONGITUDINAL CONTROL







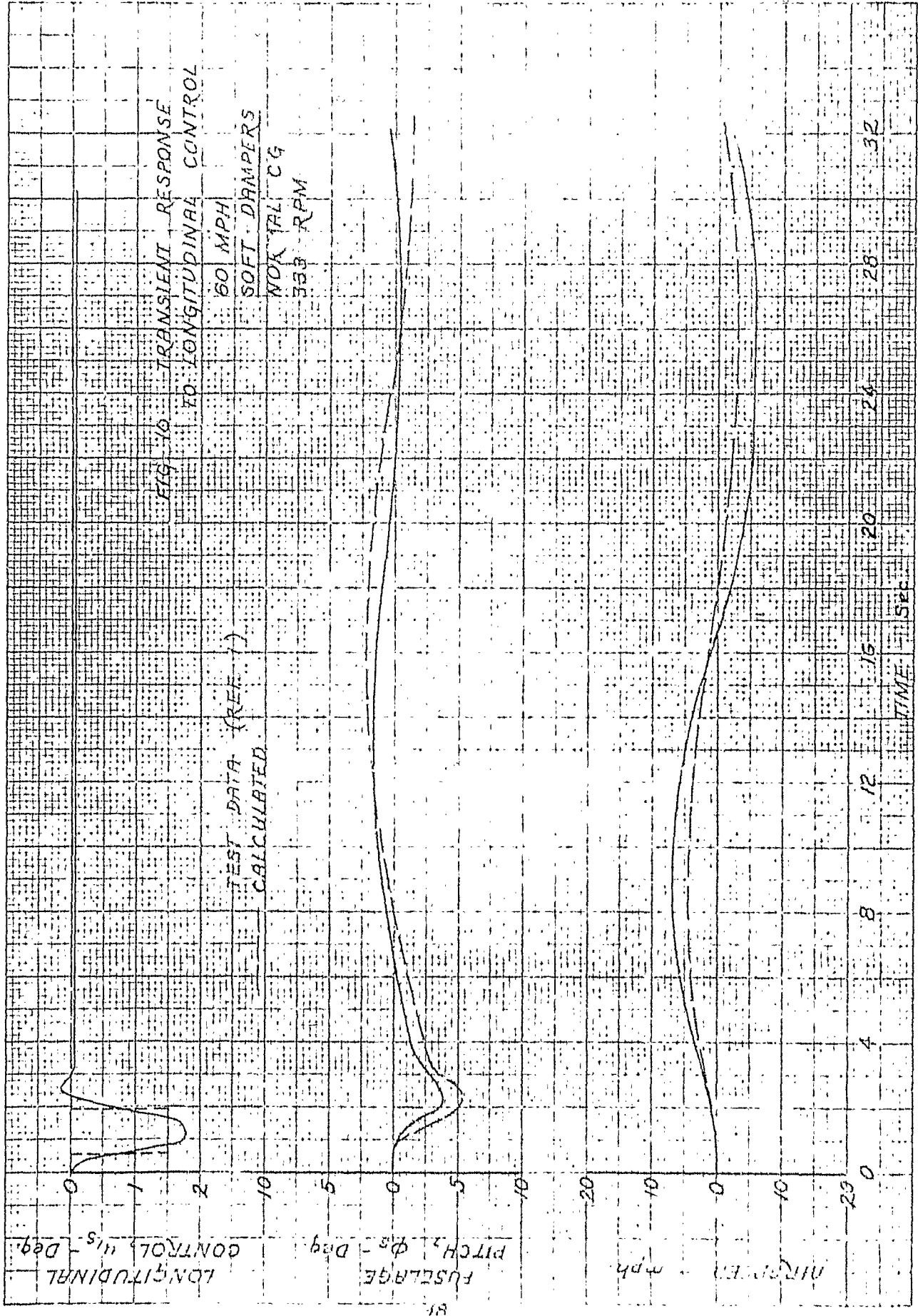


FIG. 10 TRANSIENT RESPONSE TO LONGITUDINAL CONTROL

32

28

24

20

16

12

8

4

0

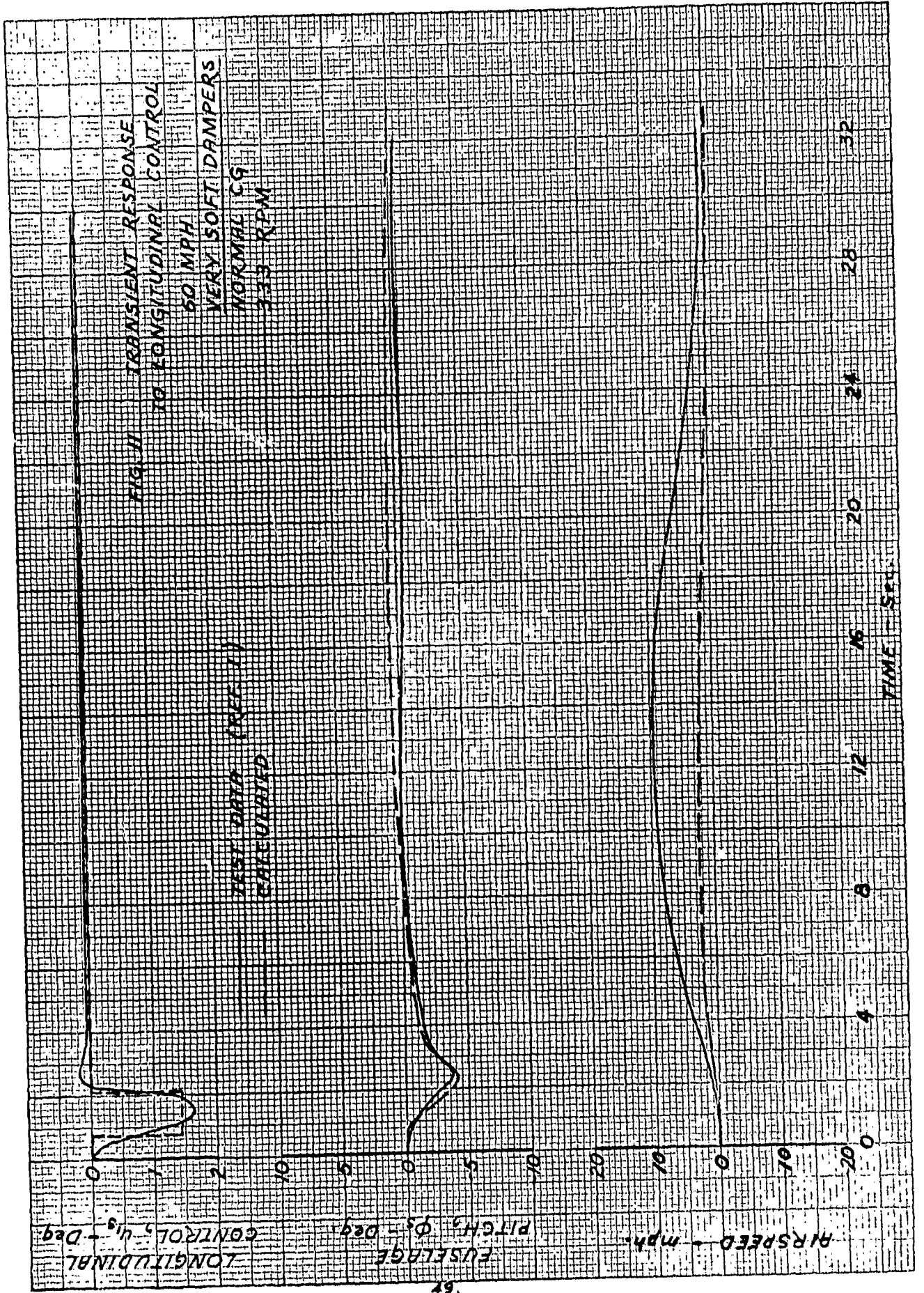


FIG. 12 FREQUENCY RESPONSE
 TO LONGITUDINAL CONTROL
 20 MPH - 61 AIRSPEED RESPONSE

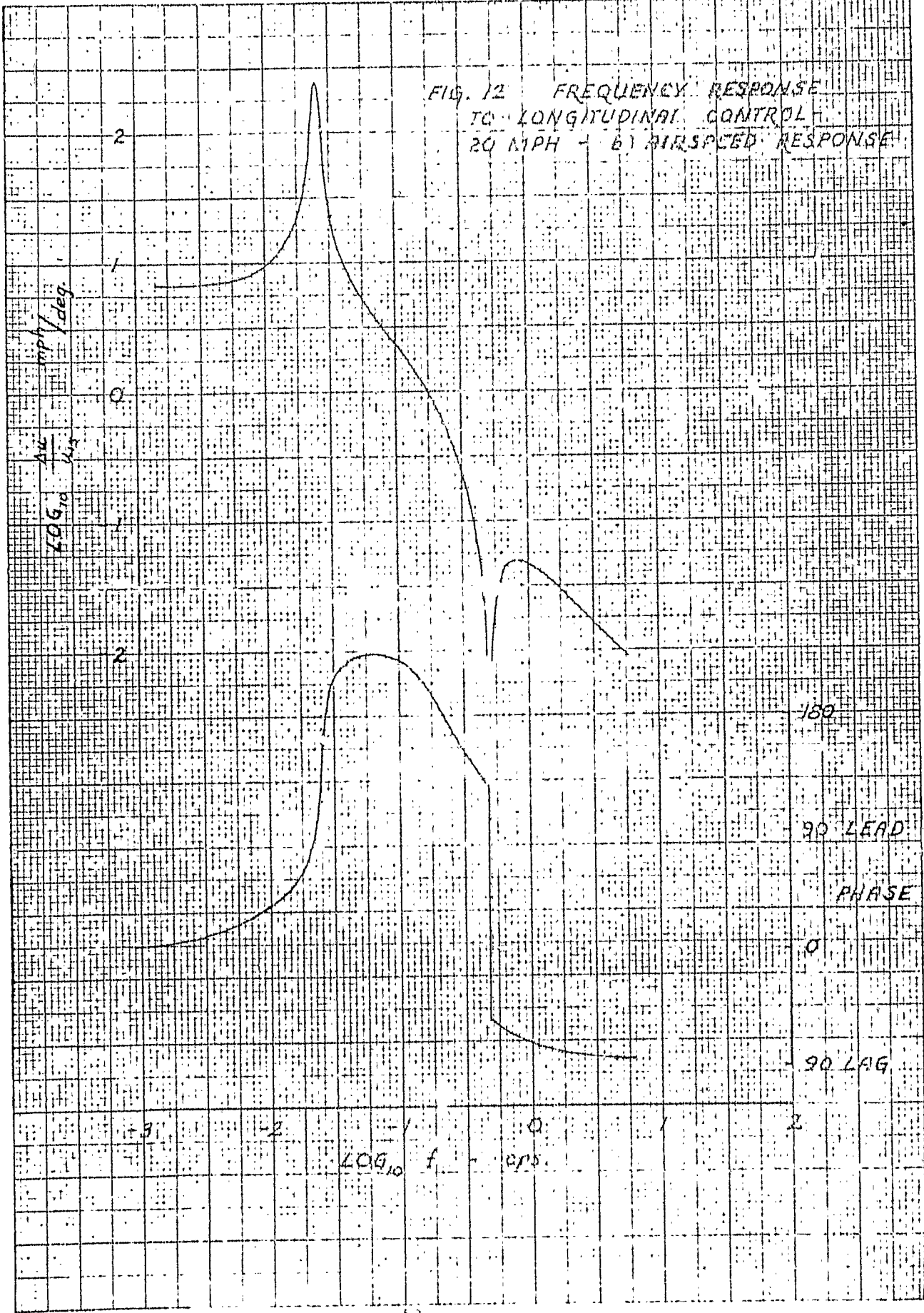


FIG. 12 FREQUENCY RESPONSE
 TO LONGITUDINAL CONTROL -
 20 MPH - a) PITCH RESPONSE

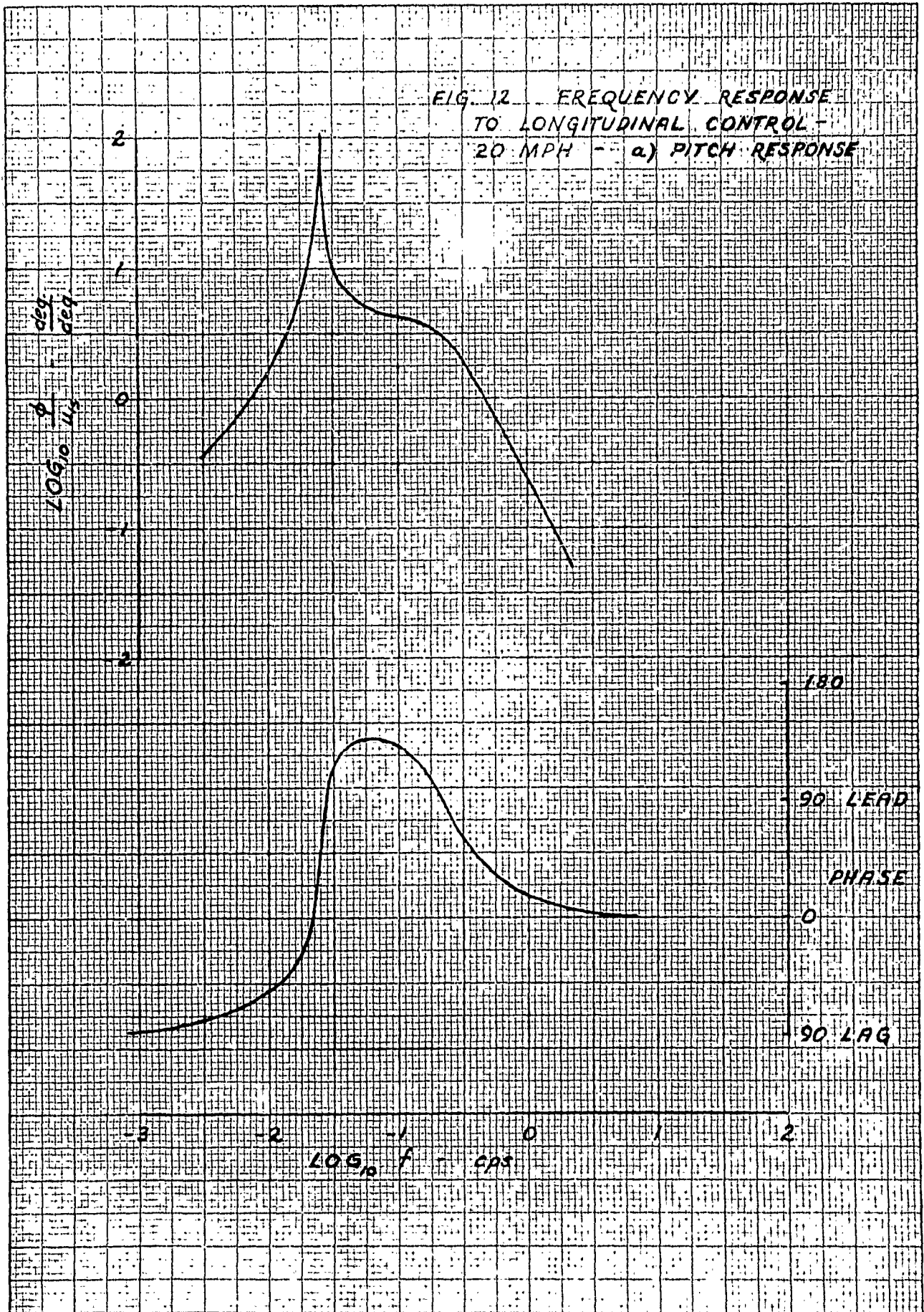


FIG. 13 FREQUENCY RESPONSE
 TO LONGITUDINAL CONTROL -
 40 MPH - a) PITCH RESPONSE

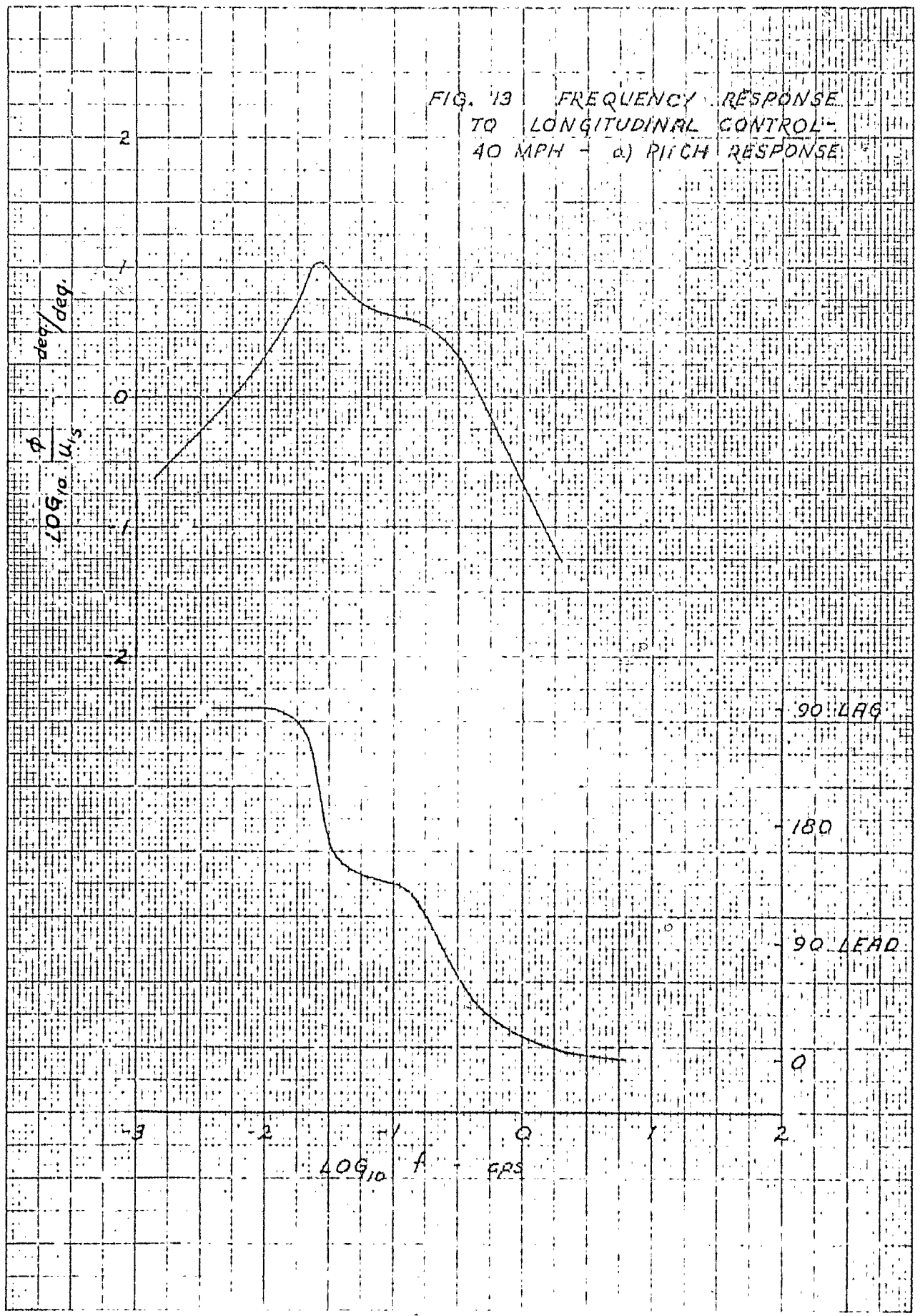


FIG. 13. FREQUENCY RESPONSE
 TO LONGITUDINAL CONTROL
 40 MPH - b) AIRSPEED RESPONSE

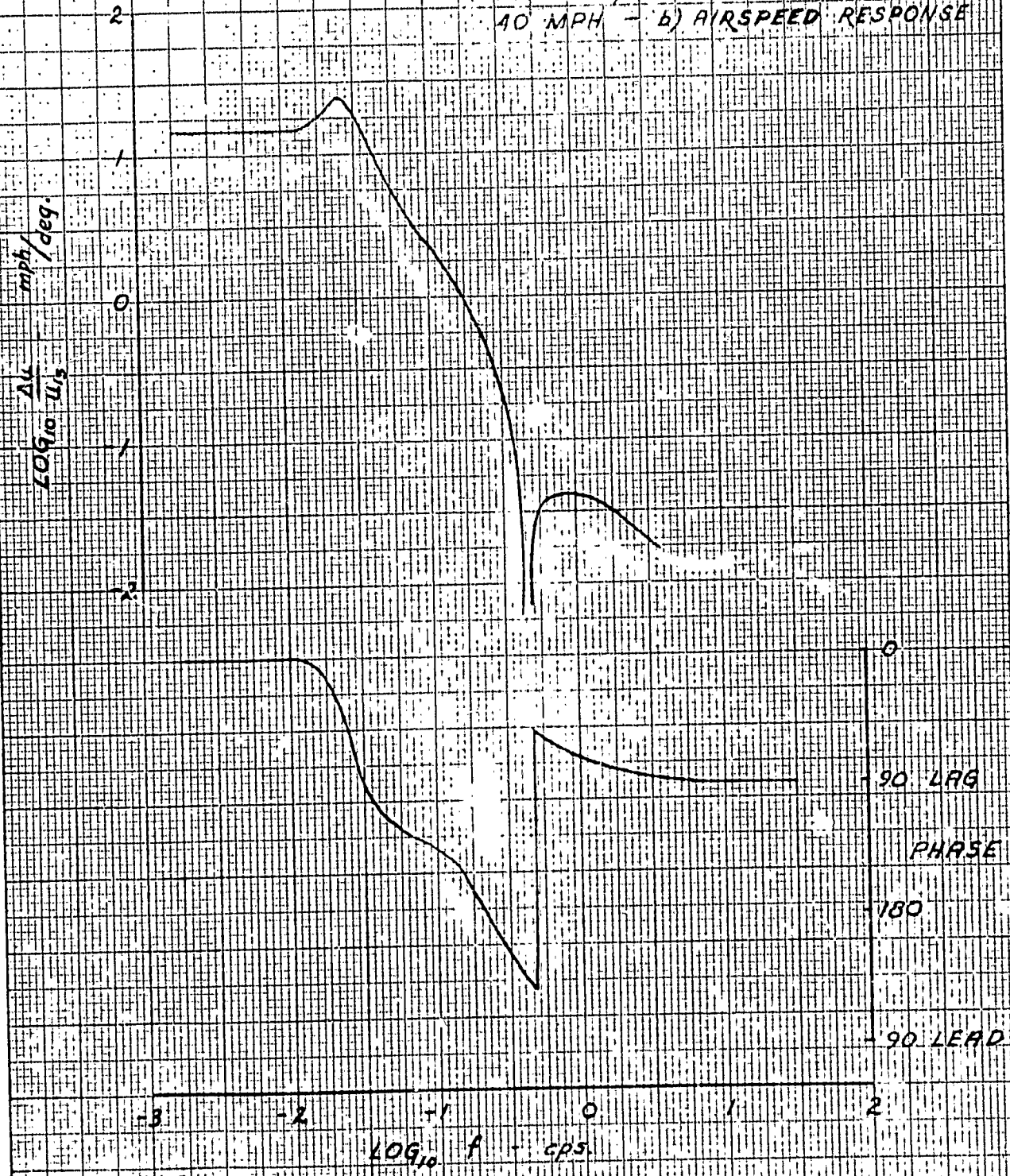


FIG. 14. FREQUENCY RESPONSE
TO LONGITUDINAL CONTROL
60 MPH - a) PITCH RESPONSE

TEST POINTS FROM
REF. 21, FIG. 4

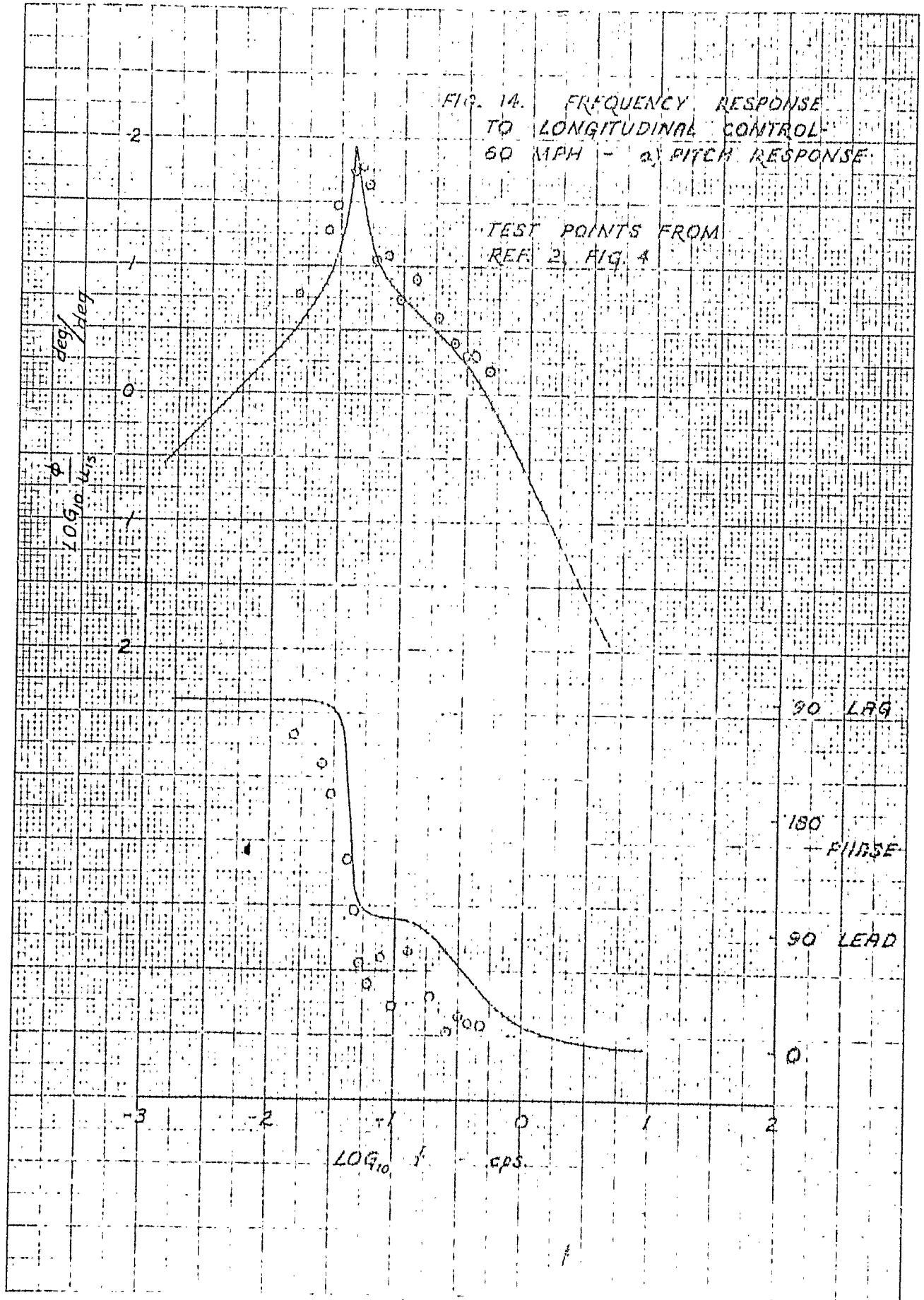


FIG. 14. FREQUENCY RESPONSE TO LONGITUDINAL CONTROL - 60 MPH - b) AIRSPEED RESPONSE

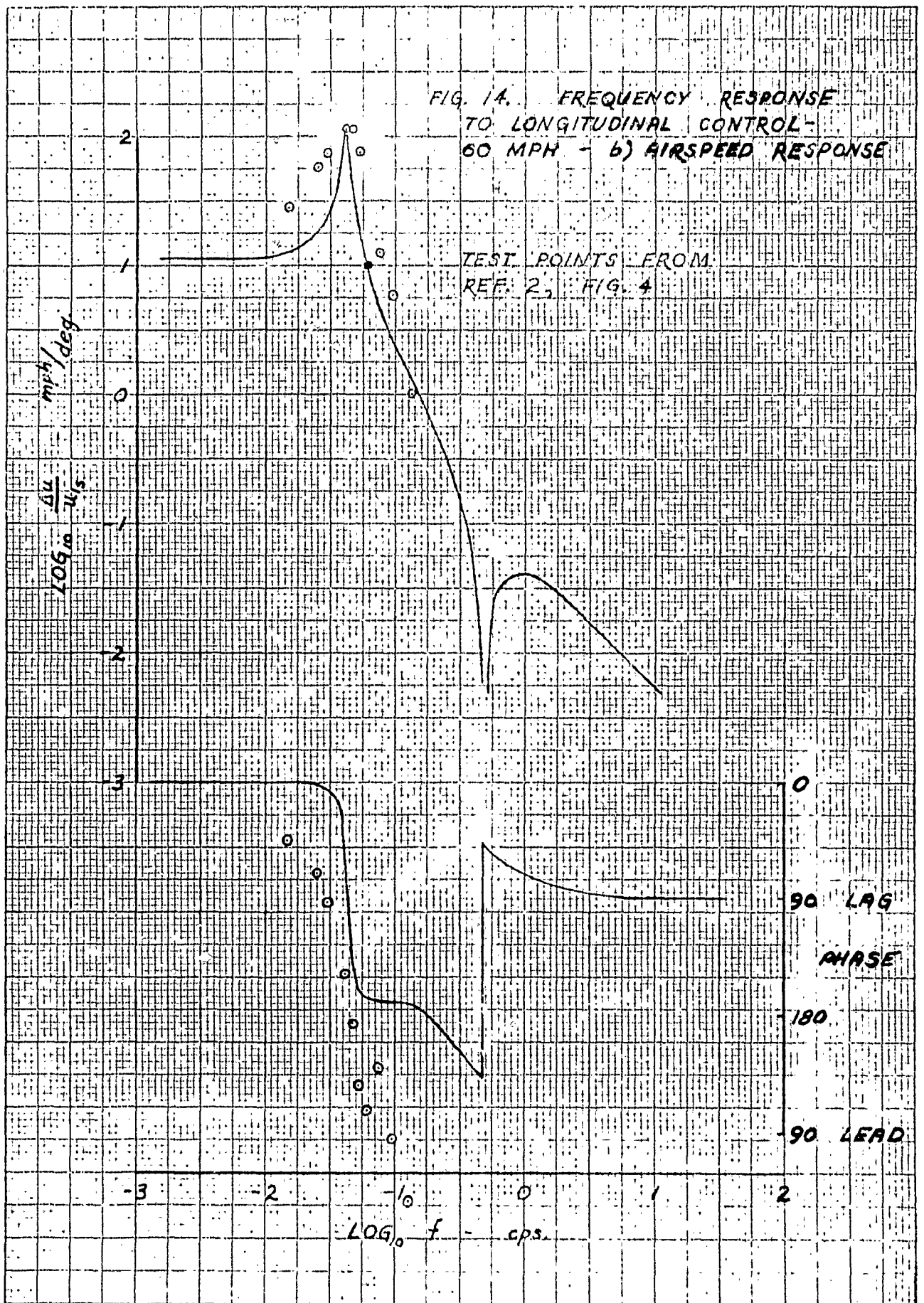


FIG. 15 FREQUENCY RESPONSE
 TO LONGITUDINAL CONTROL -
 80 MPH - (a) FITCH RESPONSE

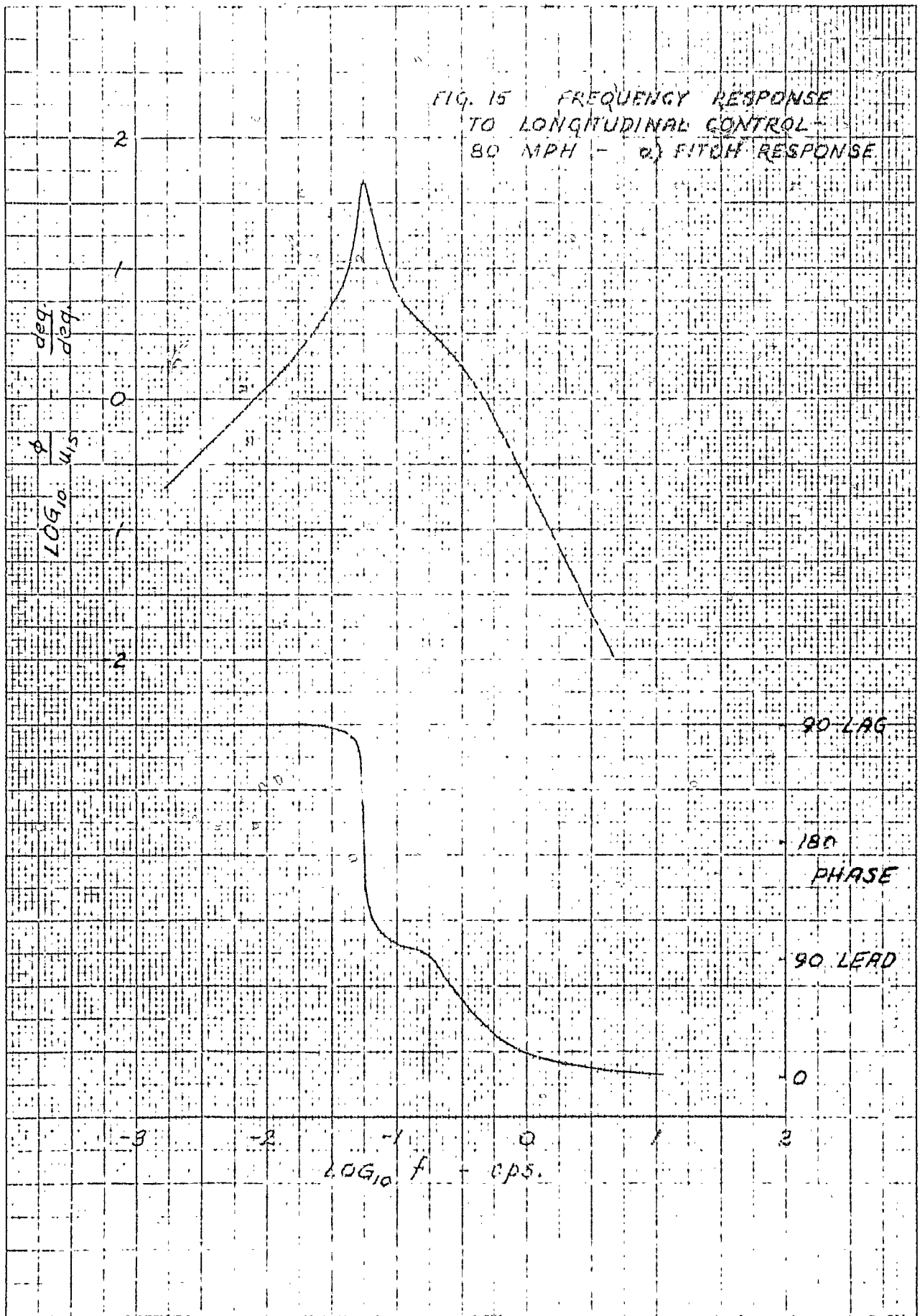


FIG. 15 FREQUENCY RESPONSE
 TO LONGITUDINAL CONTROL -
 30 MPH - b) AIRSPEED RESPONSE

